Technical Note on Quality Assessment for Jilin-1 GF02

Author(s): **_Fay Done_**
Task 1 Mission Expert

Approval: **_Fay Done_**
Task 1 Lead

Accepted: **_Clement Albinet_**
EDAP Technical Officer

EDAP.REP.050 _Issue: 1.0_ _13 04 2022_

TABLE OF CONTENTS

AMENDMENT RECORD SHEET

The Amendment Record Sheet below records the history and issue status of this document.

ISSUE	DATE	REASON
0.1	21 01 2022	First draft for ESA review
1.0	13 04 2022	First issue

1. EXECUTIVE SUMMARY

The Jilin-1 constellation of Earth Observation (**EO**) satellites, operated by **Chang Guang Satellite Technology Company** (China), consists of the optical **Jilin-1 GF02A** (launched November 2019) and **B** (launched December 2019) twin satellites. These twin satellites provide users with Very High Resolution (**VHR**) multispectral (**MS**) and panchromatic (**PAN**) mono and stereo imagery of the Earth's surface.

The results of the assessments performed on the sample of **orthorectified bundle** products, procured from the data provider, **Head Aerospace,** between April and September 2021, are summarised in Table 1-1.

Table 1-1: Mission Jilin-1 GF02: Assessment Area Results

Assessment Area	Results
GF02 A / B Ground Sampling Distance / Pixel Size @ Nadir: Panchromatic: 0.75 m. Multispectral: 3.0 m.	
Geometric Calibration Quality	**1. Absolute Geolocation Accuracy** The results of this assessment indicate the (average) absolute geolocation accuracy of orthorectified multispectral and panchromatic imagery is 12.94 m and 5.12 m CE90, respectively. Therefore, the minimum performance requirement specified by the operator as < 20.0 m CE90 [RD-7] has been met. **2. Temporal Geolocation Accuracy** The temporal geolocation accuracy could not be assessed due to the very small sample of suitable products procured. Note a minimum performance requirement has not been specified by the operator for this metric. **3. Band Co-registration Accuracy** The results of this assessment indicate the band co-registration accuracies of the multispectral band pairs (blue-green, green-red and red-near-infrared) is 0.44, 0.52 and 0.67 multispectral pixels CE90, respectively. The band co-registration accuracies of the multispectral-panchromatic band pairs (near-infrared-panchromatic) is 2.37 CE90 multispectral pixels. The latter results are associated with a small error budget (i.e. error associated with the method). Note a minimum performance requirement has not been specified by the operator for this metric.

Radiometric Calibration Quality	**1. Absolute Radiometric Accuracy** The results of this assessment indicate the data is poorly calibrated (absolute radiometric accuracy < 22 %) and the reason(s) for this is not clear at this time. However, as the latter appears to be prevalent with the other Jilin-1 missions assessed, it could be due to the calibration method used and so it is recommended the operator re-assesses their calibration method. Note a minimum performance requirement has not been specified by the operator for this metric. **2. Temporal Radiometric Accuracy** The temporal radiometric accuracy could not be assessed due to the very small sample of suitable products procured. Note a minimum performance requirement has not been specified by the operator for this metric.
Image Quality	**1. Modulation Transfer Function** This assessment could not be performed as the tool used could not accurately detect or define the edges of the chosen artificial modulation transfer function target (i.e. blurring is evident, poor sharpness indicates degradation of image quality). This may be because the modulation transfer function compensation correction had not been applied during processing, as indicated in the product metadata (this parameter is not sufficiently detailed in [RD-3]). Note a minimum performance requirement has not been specified by the operator for this metric. **2. Signal-to-Noise Ratio** The results of this assessment indicate the signal-to-noise ratio is relatively good for all bands, where the range is 85 – 220:1. Note a minimum performance requirement has not been specified by the operator for this metric. **3. Image Interpretability** The results of this assessment indicate the interpretability of this imagery is reasonable (i.e. features or objects of interest can be interpreted) but there is room for improvement (e.g. deblurring). Note a minimum performance requirement has not been specified by the operator for this metric.

Visual Inspections	The results of this assessments indicate there are no anomalies or artefacts present in the products procured.

2. INTRODUCTION

This technical note details the results of the (preliminary) mission data quality assessments (including geometric calibration, radiometric calibration and image quality) performed on a sample of orthorectified bundle products generated for Jilin-1 GF02A and B, a relatively new addition to Head Aerospace's EO portfolio of commercial optical missions.

The aforementioned mission data quality assessments are performed in accordance with the assessment guidelines, detailed in [RD-1 RD-2], which constitute the European Space Agency (**ESA**) Earthnet Data Assessment Pilot (**EDAP**) Project's EO Mission Data Quality Assessment Framework. An important representation of the latter framework, constructed by the National Physical Laboratory (**NPL**, U.K), is what is known as the maturity matrix. It is a diagrammatic summary of the following:

- **Documentation Review**: the EDAP optical team reviews materials (e.g. data and documentation) provided by the mission provider (data provider and / or operator), some of which may not be publicly available, or even the scientific community (e.g. published papers). The results are detailed in Section 3 (covering the first four columns of the maturity matrix, see Table 3-1).

- **Data Quality Assessments**: the EDAP optical team performs the data quality assessments (i.e. validation assessments), independently of any validations performed by the mission provider. The results are detailed in Section 4 (covering the last column of the maturity matrix, see Table 3-1).

The above assessments are performed by the project's optical team using the appropriate in-house and open-source ad-hoc scripts / tools.

It is important to note that the purpose of the EDAP EO Mission Data Quality Assessment Framework is to ensure that the delivered commercial mission data is fit for purpose and that all decisions regarding the inclusion of the commercial mission as an ESA third party mission can be made fairly and with confidence.

2.1 Reference Documents

The following is a list of reference documents with a direct bearing on the content of this proposal. Where referenced in the text, these are identified as [RD-n], where 'n' is the number in the list below:

RD-1. EDAP Best Practice Guidelines, EDAP.REP.001, v1.2, September 2019.

RD-2. Earth Observation Mission Quality Assessment Framework – Optical Guidelines, EDAP.REP.002, v2.0, December 2020.

RD-3. Chang Guang Satellite Technology Co Ltd. - Jilin-1 Imagery Product Guide, v1.1, April 2021.

RD-4. Head Aerospace – Introduction to the Jilin-1 Satellites and Products, v0.1 (Draft), May 2020.

RD-5. Jilin-1 Satellites Radiometric Calibration (not publicly available and no other document information provided)

RD-6. Wilkinson, M.D., Dumontier, M., Aalbersberg, I.J., Appleton, G., Axton, M., et al. 2016. The FAIR Guiding Principles for scientific data management and stewardship. Scientific Data 3, 160018. (doi:10.1038/sdata.2016.18)

RD-7. Head Aerospace – Jilin Stereo (GF02A/B) Data Sheet, v1.0, 2020.

RD-8. Zanoni, "IKONOS Signal-to-Noise Ratio Estimation", March 25-27, 2002, JACIE Workshop, 2002 https://ntrs.nasa.gov/search.jsp?R=20040004380

RD-9. National Image Interpretability Rating Scales, https://fas.org/irp/imint/niirs.htm

RD-10. M. Cournet, A. Giros, L. Dumas, J.M. Delvit., D. Greslou, F. Languille, G. Blanchet, S. May, and J. Michel (2016). 2D Sub-Pixel Disparity Measurement Using QPEC / Medicis, Int. Arch. Photogramm. Remote Sens. Spatial Inf. Sci., XLI-B1, 291-298, doi: 10.5194/isprs-archives-XLI-B1-291-2016.

RD-11. SPOT Image Quality Performances, CNES C443-NT-0-296-CN, https://www.intelligence-airbusds.com/files/pmedia/public/r438_9_spot_quality_performances_2013.pdf

RD-12. Sentinel-2 MPC L1C Data Quality Report, S2-PDGS-MPC-DQR, Issue 71, 03/01/2022. https://sentinel.esa.int/documents/247904/685211/Sentinel-2_L1C_Data_Quality_Report

RD-13. Department of the Interior U.S. Geological Survey, Landsat 8 (L8) Data Users Handbook, LSDS-1574, Version 5.0, https://prd-wret.s3-us-west-2.amazonaws.com/assets/palladium/production/atoms/files/LSDS-1574_L8_Data_Users_Handbook-v5.0.pdf

2.2 Glossary

The following acronyms and abbreviations have been used in this Report.

BOA	Bottom-of-Atmosphere
CEOS	Committee for Earth Observing Satellites
DGPS	Differential Global Positioning System
EDAP	Earthnet Data Assessment Pilot
EO	Earth Observation
ESA	European Space Agency
ESF	Edge Spread Function
FAIR	Findable, Accessible, Interoperable and Reusable
GCP	Ground Control Points

IVOS	Infrared and Visible Optical Sensors
MS	Multispectral
MTF	Modulation Transfer Function
NIIRS	National Imagery Interpretability Rating Scale
NPL	National Physical Laboratory
PAN	Panchromatic
PICS	Pseudo-invariant Calibration Site
PHR	Pleaides High-Resolution
POI	Points of Interest
PSF	Point Spread Function
SNR	Signal-to-Noise Ratio
TOA	Top-of-Atmosphere
VHR	Very High Resolution
WGCV	Working Group for Calibration and Validation

3. EDAP QUALITY ASSESSMENT

3.1 EDAP Maturity Matrix

Table 3-1 Maturity Matrix for Jilin-1 GF02

Product Information	Product Generation	Ancillary Information	Uncertainty Characterisation	Validation
Product Details	Sensor Calibration & Characterisation Pre-flight 🔒	Product Flags	Uncertainty Characterisation Method	Reference Data Representativeness
Product Availability & Accessibility	Sensor Calibration & Characterisation Post-Launch 🔒	Ancillary Data	Uncertainty Sources Included 🔒	Reference Data Quality
Product Format 🔒	Additional Processing 🔒		Uncertainty Values Provided 🔒	Validation Method
User Documentation			Geolocation Uncertainty 🔒	Validation Results
Metrological Traceability Documentation				

Key
Not Assessed
Not Assessable
Basic
Good
Excellent
Ideal
🔒 Not Public

3.1.1 Product Information

Product Details	
Product Name	*Jilin-1 GF02A/B Orthorectified Bundle Product (L3A)*
Sensor Name	*Jilin-1 GF02A/B*
Sensor Type	*(Pushbroom) Optical – Multispectral and Panchromatic* *Panchromatic: 450 - 800* *Blue: 450 - 510* *Green: 510 - 580* *Red: 630 – 690* *Near-infrared: 770 - 895*
Mission Type	*Twin satellites*
Mission Orbit	*Jilin-1 GF02A/B: Sun-synchronous: 535 km altitude, local time descending node 10:00am*
Product Version Number	*(Not specified.)*
Product ID	*JL1GF02A_PMS01_20200707180240_200027911_103_0021_001_L3A* *Satellite Name (JL1GF02x: A or B), Detector Name and Number (PMS0x: 1 – 2), Imaging Time (YYYYMMDDHHMMSS (Beijing Local)), Mission Planning Number, Segment Number, Scene Number, Production Times, Product Level.*
Product Processing Level	*Level 3A (Standard Orthorectified)* *System geometric correction product. Fine DEM data is used for orthocorrection on the basis of L1 products. Used for practical applications such as feature extraction, classification, drawing, etc. It is suitable for users who have higher requirements for precision. (Note: SRTM90 is used as reference for elevation correction)*
Measured Quantity Name	*Digital Numbers (DN) / Spectral Radiance*
Measured Quantity Units	*DN (12-bit scaled to16-bit) / W.st^{-1}.m^{-2}.μm^{-1}*
Stated Measurement Quality	*Radiometric Quality: Not specified.* *Geometric Quality: 20 m CE90 @ Nadir?*
Spatial Resolution	*Very High Resolution* *Multispectral: 2.00 m* *Panchromatic: 0.50 m* *Standard scene size (at Nadir) 21.5 km x 21.5 km*
Spatial Coverage	*Global (Orbital Inclination ?),Swath Width: > 40 km*
Temporal Resolution	*Revisit < 2 Days (Latitude Dependent)*
Temporal Coverage	*Mission Lifetime > 3 Years (Launched 11/2019)*
Point of Contact	*Head Aerospace*
Product locator (DOI/URL)	-
Conditions for access and use	*contact@head-aerospace.fr*

Limitations on public access	*The sensor products are made available upon request (orders / tasks are placed with the data provider's imagery support team: contact@head-aerospace.fr) or through their online catalogue (https://headfinder.head-aerospace.eu/pub).*
Product Abstract	*Jilin-1GF02A launched on November 13, 2019, and Jilin-1GF02B on December 7, 2019. The two satellites are the first of next-generation satellites providing high-resolution series push-broom imaging capacity. They are operated together with two other Jilin-1 satellites, EarthScanner (JL1-KF01A) and Jilin GXA, which offer daily revisit at 0.75 m range resolution. These two Jilin-1 Stereo satellites offer 0.75 m resolution with 40 km swath, agile satellites for stereo imaging and large area mapping. The satellite adopts the long focal length optical dual camera with common reference alignment. The technology combines dual-frequency GNSS orbit determination and high-precision dual-satellite sensitive attitude determination technology. [RD-7]*

Availability & Accessibility	
Grade: Good *Justification: The products and their content are compliant with many of the Findable, Accessible, Interoperable and Reusable (**FAIR**) Data Principles [RD-6] for scientific data management and stewardship. The data is available to users, at cost, through an easy-to-access commercial license.*	
Compliant with FAIR Principles	*The products and their content are compliant, and where applicable, with many of the FAIR Data Principles for scientific data management and stewardship. It is recommended, however, to have the data be released with a clear and accessible data usage licence.*
Data Management Plan	*This is not shared by the data provider.*
Availability Status	*As mentioned previously, the products are made available upon request (orders / tasks are placed with the data provider's imagery support team: contact@head-aerospace.fr) or through their online catalogue (https://headfinder.head-aerospace.eu/pub).*

Product Format
Grade: Good
Justification: The product format and content, in which standard file formats and naming conventions are generally used, is only partially described in [RD-3]; product metadata file format and content is not fully described and product quality metadata file format and content, with valuable / useful data, is not described at all (this includes units and how the values for quality parameters are calculated / determined). *It is recommended that existing documentation be updated in order to ensure the format and contents of all products are described fully, where applicable, for full understanding of the product. It is also recommended, for ease of use by the user, that timestamps (in product name and metadata) are not given in Beijing Local Time but in UTC.* *The data is not considered as analysis ready data (e.g. Committee for Earth Observing Satellites (**CEOS**) Analysis Ready Data, https://ceos.org/ard/).*

Product File Format	*The product format ensures the following imagery and metadata files, adopting standard file formats (i.e., includes: •Product Image (.TIF) •Product Image Metadata (.XML) •Product Image Quality Metadata (.XML) •Product Browse Image Icon (.JPG) •Product Browse Image Icon Thumbnail (.JPG) The product format applies to the main product type procured for these assessments (i.e. L3A) but deviations to this product format exist for products of a different type (i.e. L1).*
Metadata Conventions	*Not implemented as optional (e.g. Geographic Information – Metadata ISO).*
Analysis Ready Data?	*No (N/A)*

User Documentation		
Grade: Basic *Justification: The product user guides, provided upon request to the data provider, contains high-level information only (e.g. basic description of sensor, product type and processing level, and spectral information and instructions that allows users to convert data from digital numbers to top-of-atmosphere reflectance). The product user guide or any other available documentation does not include algorithm theoretical basis document-type information. Therefore, the status of this section of the maturity matrix has been graded as "Basic".*		
Document	Reference	QA4ECV Compliant
Product User Guide (Chang Guang)	*[RD-3]*	No
Product User Guide (Head Aerospace)	*[RD-4]*	No
Data Sheet	*[RD-7]*	No
Algorithm Theoretical Basis Document	*Documentation not made available.*	N/A

Metrological Traceability Documentation	
Grade: Not assessable.	
Document Reference	-
Traceability Chain / Uncertainty Tree Diagram Available	*Document not made available.*

3.1.2 Product Generation

Sensor Calibration and Characterisation – Pre-Launch
Grade: Basic *Justification: There is very basic information (i.e. stated values and not methodology used) provided on pre-launch radiometric calibration and characterisation, using the radiometric and spectral calibration test platform of Chang Guang Satellite Technology, only. As there is no information on pre-launch spectral or spatial calibration and characterisation activities, this section of the maturity matrix has been graded as 'Basic'.*

Summary	*This document provides high-level information on the radiometric calibration of all sensors within the Jilin-1 constellation. However, the document is not made available to users.*
References	*[RD-5] Documentation not made available to users.*

Sensor Calibration and Characterisation – Post-Launch	
Grade: Basic *Justification: There is very basic information (i.e. stated values and not the methodology used) provided on post-launch radiometric calibration and characterisation, using primarily cross-calibration methods, only. As there is no information on post-launch spectral or spatial calibration and characterisation activities, this section of the maturity matrix has been graded as 'Basic'.*	
Summary	*This document provides high-level information on the radiometric calibration of all sensors within the Jilin-1 constellation. However, the document is not made available to users.*
References	*[RD-5] Documentation not made available to users.*

Additional Processing	
Grade: Basic *Justification: There is no documentation on the processing steps carried out for orthorectification, apart from the brief mention of the use of the NASA Shuttle Radar Topographic Mission 90 m spatial resolution at equator (STRM90 Digital Elevation Model), and so this section of the maturity matrix has been graded as 'Basic'.*	
Summary	*Orthorectification*
Reference	*-*

3.1.3 Ancillary Information

Ancillary Data	
Grade: Basic *Justification: The key ancillary data required to define measurement data does not include, importantly, the following:* • *The viewing angle of the acquisition; the operator has advised that the roll angle can be used as the viewing angle, however, this is not strictly true as the viewing angle needs to take into account the pitch angle (the latter is only true when the pitch angle equals zero).* • *The uncertainties associated with measurement data (where applicable).* *Therefore, this section of the maturity matrix has been graded as 'Basic'.*	
Description	*There is some product-specific ancillary data (e.g. viewing and solar geometry angles, longitude, latitude, altitude), used to define measurements, can be found in product metadata and general ancillary data (e.g. in-band solar irradiance) can be found in the accompanying documentation (e.g. product guide, other documentation requested from the data provider). However, the viewing angle has not been accurately quantified and there are no uncertainties, where applicable, for or as ancillary data.*
Reference	*-*

Product Flags	
Grade: Not Assessable *Justification: These products do not contain flags, in their conventional form, and so this section of the maturity matrix has been graded as 'Not Assessable'.*	
Description	*The products do not contain flags in the conventional form (e.g. bit settings per-pixel) but they do contain quality information which can be used as flags (e.g. per product cloud content, product quality grade, etc.).*
Reference	-

3.1.4 Uncertainty Characteristics

Uncertainty Characterisation Method	
Grade: Not Assessable *Justification: The methods used to characterise the uncertainties associated with geometric and radiometric calibration quality are not included in the documentation made available to users, and so this section of the maturity matrix has been graded as 'Not Assessable'.*	
Description	*(see above)*
Reference	-

Uncertainty Sources Included	
Grade: Basic *Justification: There is only information / documentation concerning the sources of uncertainty related to the pre-launch radiometric calibration and characterisation of the sensor (the aforementioned radiometric calibration of Jilin-1 sensor document shared only with the EDAP team). Therefore, this section of the maturity matrix has been graded as 'Basic'.*	
Description	*(see above)*
Reference	-

Uncertainty Values Provided	
Grade: Basic *Justification: The documentation provides single uncertainty values that are used to characterise geometric performance per product and for the whole mission only but as it is not known how these uncertainty values are determined (quantified) and where they are directly applicable (i.e. at nadir (assumed here) or full range viewing angles), this section of the maturity matrix has been graded as 'Basic'.* *It is recommended the operator provides uncertainty values used to characterise the radiometric performance (e.g. absolute radiometric accuracy) for the whole mission also.*	
Description	*(see above and below)*
Reference	-

Geolocation Uncertainty

Grade: Good *Justification: A single geolocation uncertainty (i.e. geolocation accuracy) value, typically described as a circular error is provided for the whole mission and a single geolocation uncertainty value is provided per product (found in the quality metadata file as <GeoPrecision> but this is an assumption as the product guide does not provide any detail on this parameter) and so this section of the maturity matrix has been graded as 'Good'. Note the calculation of the latter is not known.*	
Description	*The geolocation uncertainty associated with orthorectified data for this mission is < 20 m (applicable to full range of viewing angles?).*
Reference	*[RD-3, RD-7]*

3.1.5 Validation

It is important to note this section, relating to the 'Validation' column of the maturity matrix, is based on the results of the data quality assessments performed by the EDAP optical team **only** (i.e. **independently** of any data quality assessments performed by the data provider and / or operator).

Reference Data Representativeness	
Grade: Basic *Justification: The representativeness of the set of reference data, which refers to the extent (e.g. dynamic range, seasonal variation, geographical variation) to which reference measurements reflect the satellite measurements that they are being used to validate, is good (i.e. suitable) but the variety of reference data used (e.g. 'gold standard' reference mission sensor data, in-situ data) is relatively small, compared to what is available to the community, and so this section of the maturity matrix has been graded as 'Basic'.* *(Note, in general, increasing representativeness requires that a variety of different reference datasets, to cover different observation conditions, be used.)*	
Summary	*(See above)*
References	-

Reference Data Quality and Suitability	
Grade: Good *Justification: The reference data quality and suitability used by EDAP comes with a single uncertainty value for the entire sensor mission, and so this section of the maturity matrix has been graded as 'Good'.*	
Summary	*The data used as a reference for some of the radiometric calibration quality assessments include in-situ reference data from the well-established and documented RadCalNet.* *The data used as reference for the geometric calibration quality assessments include orthorectified panchromatic imagery from SPOT-5, which is validated by CNES as 2.5 m RMSE absolute accuracy, and ground control points derived during a field survey with an absolute accuracy of 0.1 m.* *The data used as reference for the image quality assessments include orthorectified multispectral imagery from Pléiades.*
References	*[RD-8], [RD-11]*

Validation Method	
Grade: Good *Justification: The validation methods used, despite being well-documented and used by the scientific community, produce simple uncertainty values (e.g. from a statistical distribution of results), and so this section of the maturity matrix has been graded as 'Good'.*	
Summary	*The validation methods used to assess image quality, geometric calibration and radiometric calibration quality are all well-documented and used by the scientific community.*
References	*[RD-8], [RD-9]*

Validation Results	
Grade: Good *Justification: The validation results, from validation assessment performed independently of those performed by the operator, show good agreement between satellite sensor and reference measurements (and within uncertainties), with the exception for the validation results of radiometric calibration quality, and so this section of the maturity matrix has been graded as 'Good'.*	
Summary	*The validation results of all assessments are summarised in Section 1.*
References	*See Section 4 and 5.*

4. DETAILED JILIN-1 GF02 QUALITY ASSESSMENTS

4.1 Objectives

The objectives of this work are to assess all core aspects of sensor data quality (geometric calibration, radiometric calibration, image quality) against sensor and product quality requirements or specifications, using the sample of sensor products procured.

It is important to note that for each assessment, comparisons between the two satellites cannot be performed, or reliably performed, as the sample of products procured for each one is small. Therefore, as they are twin satellites, we assume that their data quality is 'identical'.

4.2 Geometric Calibration Quality

This section describes the assessment of geometric calibration quality, implemented by the processing chain, of sensor products, detailed in Table 4-1, in terms of **absolute geolocation accuracy**, **temporal geolocation accuracy** and **band co-registration accuracy**.

Table 4-1 Geometric Calibration Quality Assessment Product Sample

Product Number	Product Name (JL1GF02x) L3A	Roll Angle / Viewing Angle (°)
1	JL1GF02B_PMS1_20210626180250_200053836_103_0001_001	19.57
2	JL1GF02B_PMS2_20210626180250_200053836_103_0001_001	19.57
3	JL1GF02A_PMS1_20210403174102_200046065_101_0002_001	-9.52
4	JL1GF02A_PMS1_20210413175418_200046999_102_0002_001	17.55
5	JL1GF02A_PMS1_20210519174421_200050263_105_0005_001	13.43

4.2.1 Absolute Geolocation Accuracy

4.2.1.1 Description and Method I (Panchromatic Imagery)

The absolute planimetric geolocation accuracy of the orthorectified panchromatic imagery is assessed using a method that directly determines the difference between the 'absolute' (actual) and apparent location of a set of ground control points (**GCP**), defined by the Differential Global Positioning System (**DGPS**)[1] during a field survey, in an image.

This assessment was performed on the following products:

La Crau (France)

[1]This field survey was conducted by ESA for contribution to the Japan Aerospace Exploration Agency's Advanced Land Observing Satellite (JAXA ALOS) optical calibration / validation activities. The accuracy of the GCPs defined by DGPS is within 0.1 m.

Product 1, 2

The orthorectified imagery included in these two products have been used to determine the geolocation accuracy of relatively low and homogenous topographies. Note the topography of La Crau does not exceed 190 m above the ellipsoid.

Piedmont (Italy)

Product 3, 4

The orthorectified imagery included in these two products have been used to determine the geolocation accuracy of *relatively high and inhomogeneous topographies,* where the 'orthorectification power' of the implemented processing is also determined. Note the topography of Piedmont does not exceed 910m above ellipsoid.

The minimum performance requirement for this metric has been specified by the operator as < 20 m (assumed to be at nadir) [RD-7]. Note it is common for the absolute geolocation accuracy to be described as a circular error at a specified percentile (e.g. CE90 means that a minimum of 90 % of the points measured have an error that is less than the stated CE90 value).

4.2.1.2 Results I

4.2.1.2.1 La Crau

The results of this assessment, detailed in Table 4-2, Figure 4-1 and Figure 4-2, indicate the aforementioned minimum performance requirement has been met; the (average) absolute geolocation accuracy of orthorectified panchromatic imagery over this region is 3.64 m RMSE and 5.12 m CE90, degraded only slightly by the observed bias (mean error, systematic error contribution) and the observed precision (standard deviation, random error contribution) in both directions. However, a more reliable / accurate result would require that more products, including more ground control points, be assessed.

Table 4-2: Absolute Geolocation Accuracy Results (La Crau)

Parameter	Product 1: Value	Product 2: Value
GCP Sample #	7	7
Mean Easting Error (m)	1.560	-2.228
Mean Northing Error (m)	1.460	2.228
Easting Error Standard Deviation (m)	2.635	2.494
Northing Error Standard Deviation (m)	1.535	1.805
Easting Root Mean Square Error (m)	3.063	3.345
Northing Root Mean Square Error (m)	2.119	2.868
Root Mean Square Error (m)	3.010	4.406
Circular Error @ 90% (m)	**5.060**	**5.170**

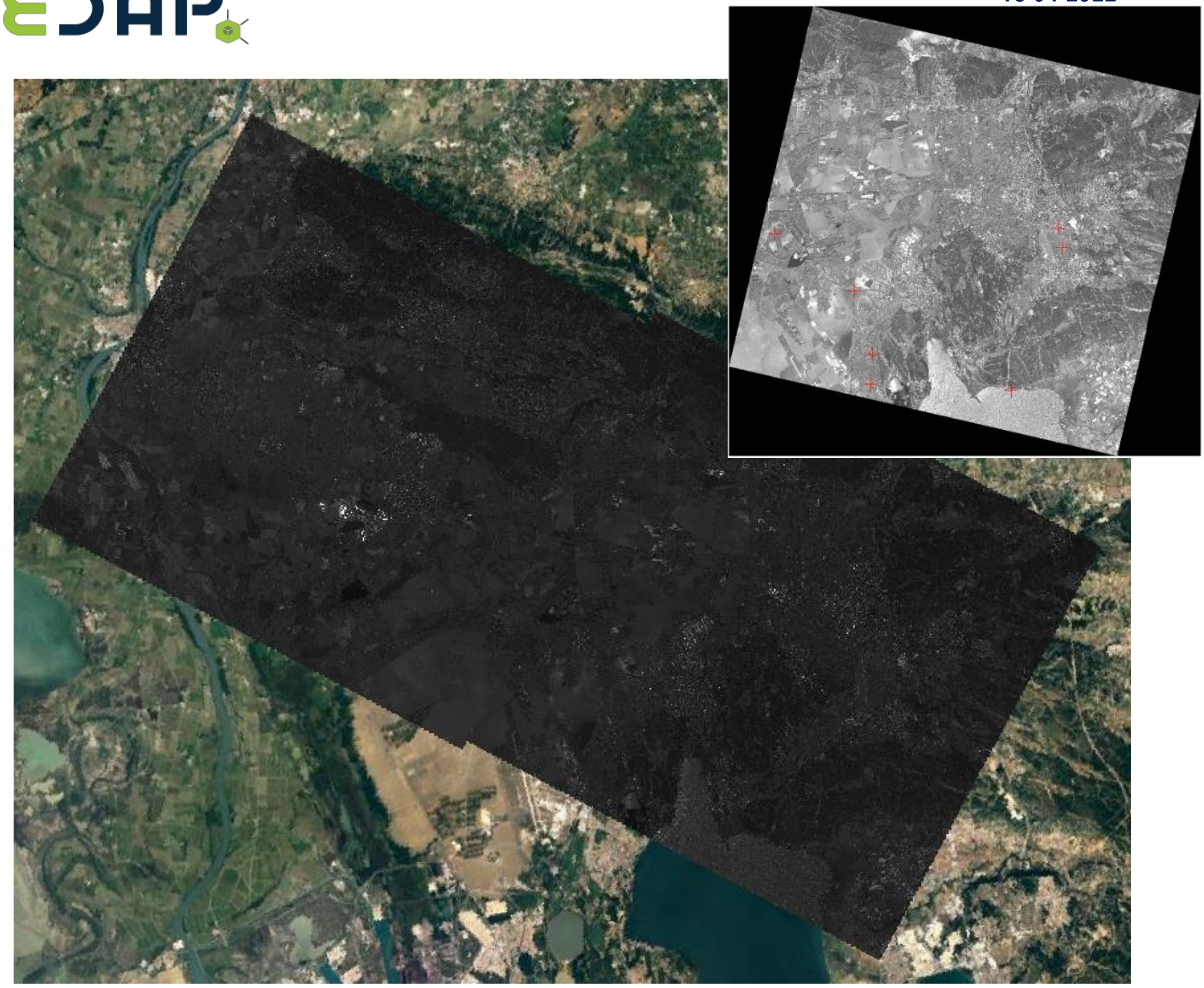

Figure 4-1; The location of product 1 and product 2 (centre) and the number, density and distribution of GCPs (+) used to determine the absolute geolocation accuracy of panchromatic imagery (top right, as an example, from product 2).

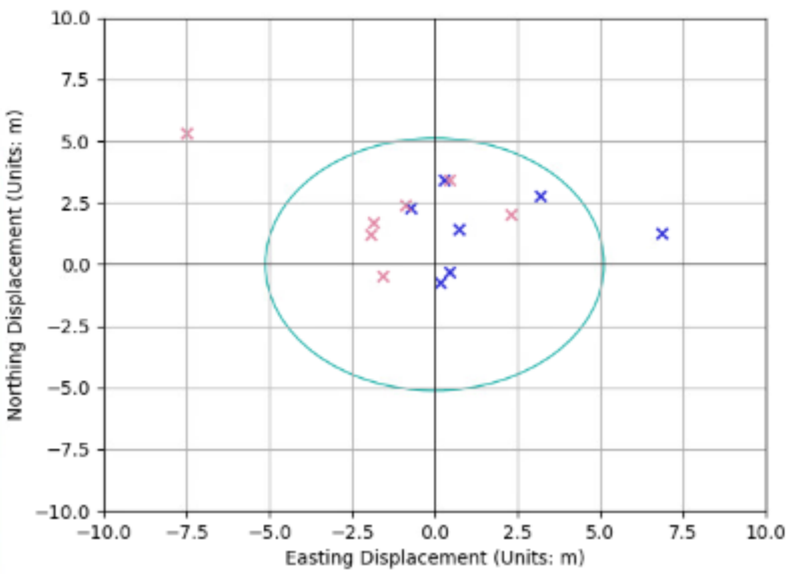

Figure 4-2: Absolute planimetric geolocation accuracy assessment on product 1 (x) and product 2 (x), and the average circular error (-) = 5.12 m).

Figure 4-2 appears to show a slight 'polarisation' of absolute geolocation accuracy, depending on the detector (product 1 from detector 1 and product 2 from detector 2 of the same acquisitions), in the easting direction. However, as mentioned previously, the assessment of more products, including more ground control points, would be needed to confirm this.

4.2.1.2.2 Piedmont

The results of this assessment, detailed in Table 4-3, Figure 4-1 4-3 and Figure 4-4, indicate the minimum performance requirement has been met; the (average) absolute geolocation accuracy of orthorectified panchromatic imagery over Piedmont is 6.95 m RMSE and 9.60 m CE90, degraded by the observed bias (mean error, systematic error contribution) and the observed precision (standard deviation, random error contribution) in both directions.

Table 4-3: Absolute Geolocation Accuracy Results (Piedmont).

Parameter	Product 3: Value	Product 4: Value
GCP Sample #	14	14
Mean Easting Error (m)	-4.079	0.011
Mean Northing Error (m)	4.861	4.163
Easting Error Standard Deviation (m)	2.812	3.488
Northing Error Standard Deviation (m)	2.286	3.719
Easting Root Mean Square Error (m)	4.954	3.488
Northing Root Mean Square Error (m)	5.371	5.582
Root Mean Square Error (m)	7.308	6.582
Circular Error @ 90% (m)	**9.532**	**9.672**

However, it is important to note the accuracy might actually be higher than that reported here as the accuracy of the ground control points used is most likely degraded due to the challenges inherent in surveying mountainous topographies.

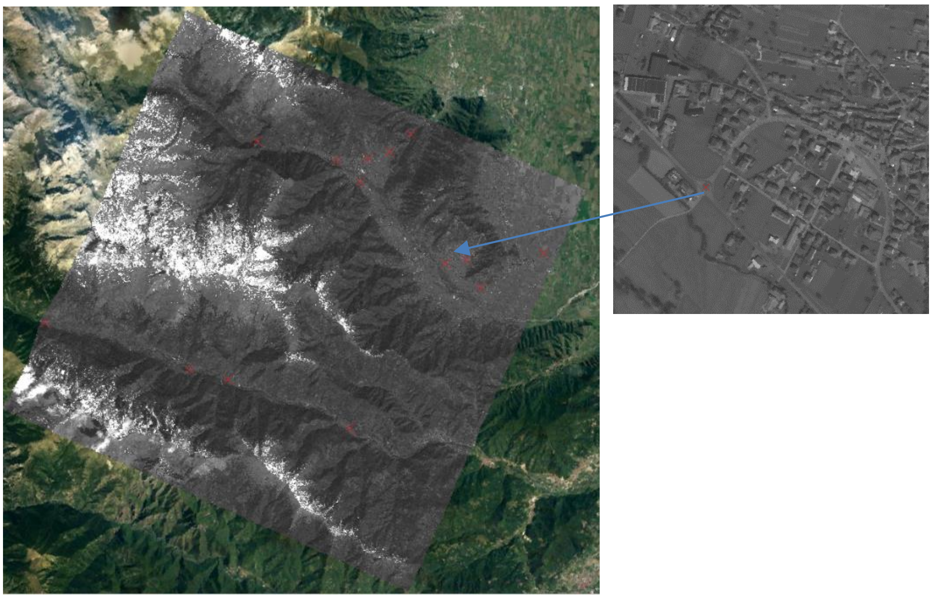

Figure 4-3 The number, density and distribution of GCPs (+) used to determine the absolute planimetric geolocation accuracy of panchromatic imagery from product 3.

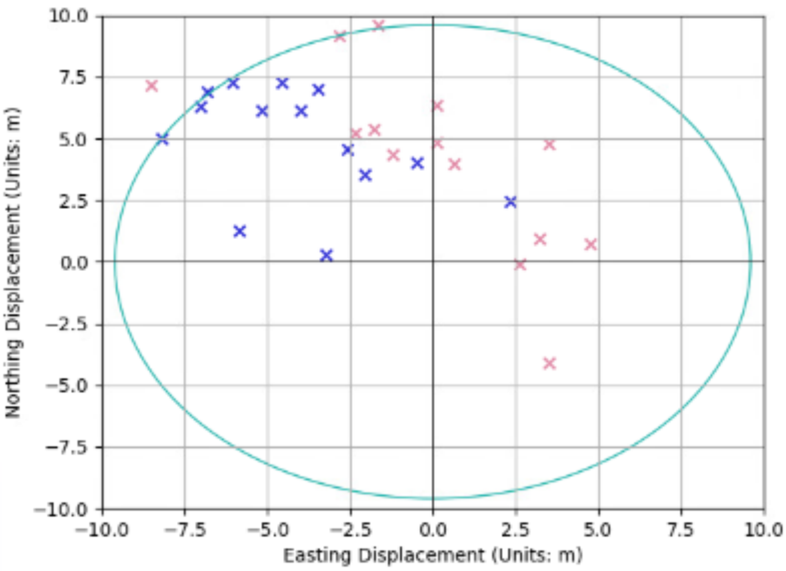

Figure 4-4: Absolute planimetric geolocation accuracy assessment on product 3 (x) and product 4 (x), and the average circular error (-) = 5.12 m).

4.2.1.3 Description and Method II (Multispectral Imagery)

The absolute planimetric geolocation accuracy of the sensor's multispectral imagery cannot be assessed using the same method adopted for the panchromatic imagery due to a lower spatial resolution (i.e. control points cannot be accurately identified). Therefore, the method used instead is one that involves the use of an image-matching tool (based on a zero-mean normalised cross-correlation algorithm, validated sub-pixel / 0.2 m accuracy), provided by the CNES MEDICIS / QPEC tool [RD-10], between the sensor's multispectral imagery and (actual) multispectral imagery from a similar sensor that has been validated for use as reference.

It is important to note, the accuracy of this tool is limited by the contrast available in the input image.

This assessment was performed on the following product:

Salon-de-Provence (France)

Product 5 (red band)

Reference Product: <SPOT 5 20121008T093232>

The reference imagery from SPOT 5 was delivered by CNES as free from systematic and non-systematic errors (i.e. due to terrain relief), and the absolute accuracy validated to be within 2.5 m (RMSE) [RD-11]; the main contributor to this slightly degraded accuracy was not the precision but actually the bias, which appeared to be systematic, of about 1.5 m. This information is of importance when using this reference imagery.

4.2.1.4 Results II

4.2.1.4.1 Salon-de-Provence

The absolute geolocation accuracy of the sensor's orthorectified multispectral imagery of Salon-de-Provence is determined by the assessment as 8.44 m RMSE and 12.55 m CE90 (detailed in Table 4-4). This absolute planimetric geolocation accuracy is very good.

Note image matching is performed at a specified confidence level (e.g. if the confidence level is specified as 95 % then the image matching results will be based on pixels that have been matched with 95% confidence / certainty).

Table 4-4: Multispectral Absolute Geolocation Accuracy Assessment Results (GF02 and SPOT 5 Image Matching CL95%)

Parameter	Product 5	
Viewing Angle (º)	13.43	
Number of Pixels	9449	
Number of Pixels Matched	804	
Mean Easting Error (m)	0.354	
Mean Northing Error (m)	1.111	
Easting Error Standard Deviation (m)	2.259	
Northing Error Standard Deviation (m)	4.466	
Easting Root Mean Square Error (m)	7.674	
Northing Root Mean Square Error (m)	3.530	
Root Mean Square Error (m)	8.447	
Circular Error @ 90% (m)	**12.550**	

The image-matching results are shown in Figure 4-5 and Figure 4-6; Figure 4-6 shows areas of concentrated high circular errors are in the hilly areas of the region and this is most likely due to the resource used to orthorectify the reference imagery originally. Note it is also important to consider the limitations of using intensity-based image matching as it includes errors originating from differences in viewing geometries, solar geometries (e.g. shadow), ground conditions (wet or dry ground), atmospheric conditions and temporal baseline between compared imagery.

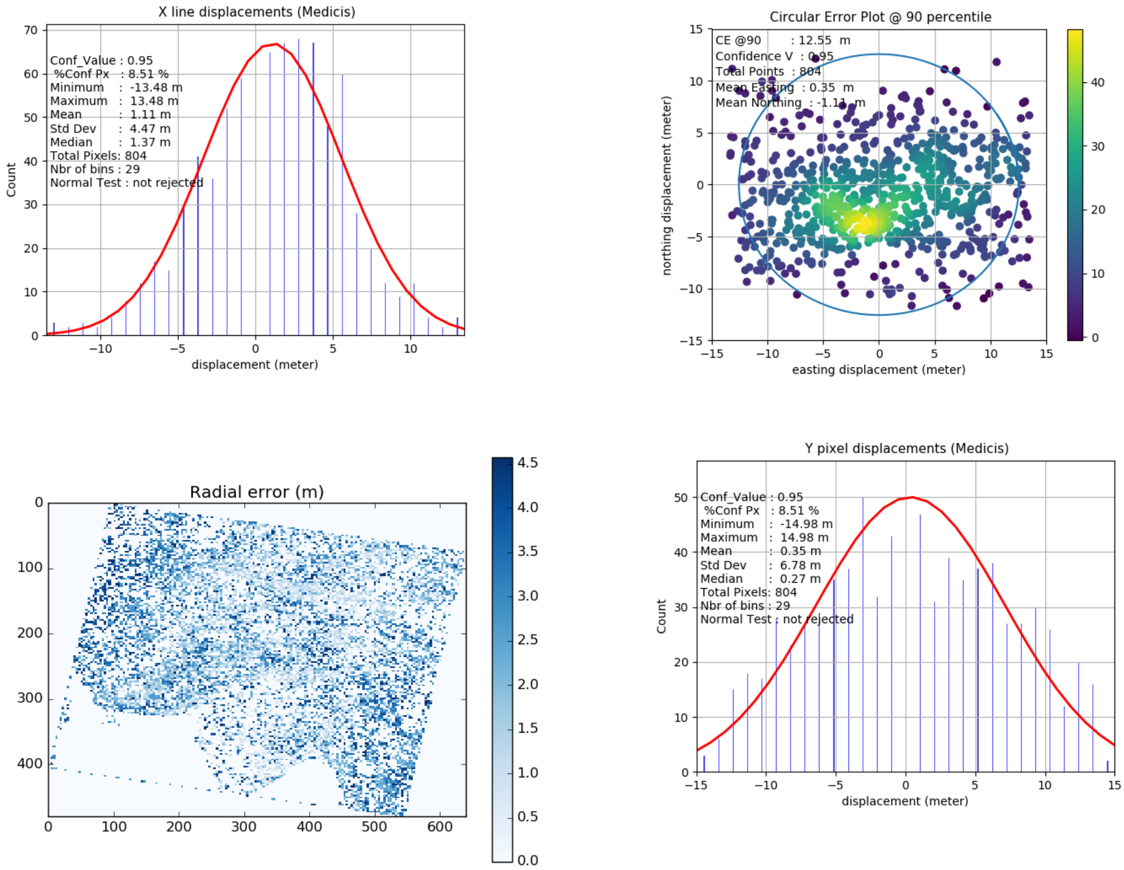

Figure 4-5: The absolute geolocation accuracy result, derived from the image matching tool, using product 5 and reference product.

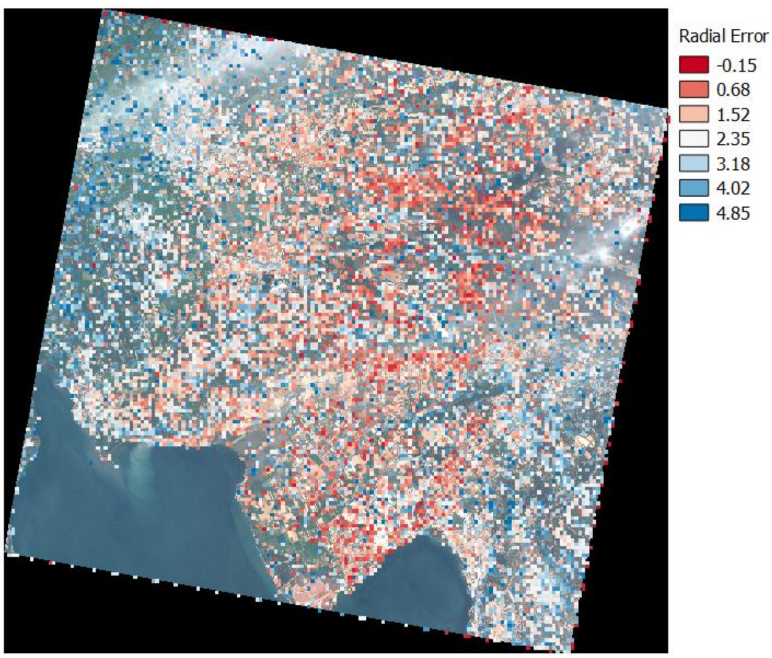

Figure 4-6: The radial error disparity layer is placed on top of the multispectral image to help identify the areas in which high radial errors are found (note no data value and radial error = 0 is transparent).

4.2.2 Temporal Geolocation Accuracy

This assessment could not be performed, as a true and meaningful time series could not be constructed from the data procured (the most suitable site had only two acquisitions, sensed only three weeks apart).

4.2.3 Band Co-registration Accuracy

4.2.3.1 Description and Method

The band co-registration accuracies have been assessed using the aforementioned image matching tool, where it was applied to the imagery of each pair of adjacent or consecutive bands (e.g. blue **(band 1)** and green **(band 2)**, green and red **(band 3)**, red and near-infrared **(band 4)**, near-infrared and panchromatic **(band 5)**, and panchromatic and blue); for any pixel location in the image space, a displacement, D, in both line (y) / pixel (x) directions is computed.

This assessment was performed on the following product(s):

Product 1, 2, 5

Note no minimum performance requirement has been specified by the data provider / operator.

4.2.3.2 Results

The results of this assessment, detailed in Table 4-5 - Table 4-7, indicate the following band co-registration accuracies (averaged for the three products assessed):

- **Multispectral Band Co-registration**
  - **Band1_2 CE@90 = 0.44 MS Pixels / 1.32 m**
  - **Band2_3 CE@90 = 0.52 MS Pixels / 1.56 m**
  - **Band3_4 CE@90 = 0.67 MS Pixels / 2.01 m**
- **Multispectral-Panchromatic Band Co-registration**
  - **Band4_5 CE@90 = 2.37 MS Pixels / 7.11 m**

(Prior to starting the assessment, the pixel size of the panchromatic imagery is downsampled, using a cubic resampling kernel, to match that of the multispectral imagery.)

Table 4-5 Product 1: La Crau: Multispectral Band Co-registration Accuracy (Image Matching Confidence Level @ 99 %). Units: Multispectral Pixels.

	Multispectral			
	Band Pair: 1_2	Band Pair: 2_3	Band Pair: 3_4	Band Pair: 4_1

# Matched Pixel Total	6011/22602	5042/22431	241/8732	99/8359
Mean Easting Error (px)	-0.03	0.09	0.03	-0.25
Mean Northing Error (px)	0.19	0.32	-0.07	0.47
Easting Error Standard Deviation (px)	0.26	0.24	0.29	1.06
Northing Error Standard Deviation (px)	0.15	0.20	0.28	0.71
Easting Root Mean Square Error (px)	0.26	0.26	0.29	1.09
Northing Root Mean Square Error (px)	0.24	0.38	0.29	0.85
Root Mean Square Error (px)	0.36	0.46	0.41	1.38
CE90 (px / m)	**0.53/1.58**	**0.65/1.94**	**0.63/1.91**	**2.17/6.50**

Table 4-6 Product 2: La Crau: Multispectral Band Co-registration Accuracy (Image Matching Confidence Level @ 99 %). Units: Multispectral Pixels.

	Multispectral			
	Band Pair: 1_2	Band Pair: 2_3	Band Pair: 3_4	Band Pair: 4_1
Product 2				
# Matched Pixel Total	7912/23984	6181/23756	302/10894	84/8033
Mean Easting Error (px)	-0.40	0.09	0.05	0.029
Mean Northing Error (px)	-0.08	-0.06	0.04	0.078
Easting Error Standard Deviation (px)	0.23	0.24	0.33	0.76
Northing Error Standard Deviation (px)	0.13	0.17	0.24	0.62
Easting Root Mean Square Error (px)	0.46	0.26	0.33	0.76
Northing Root Mean Square Error (px)	0.15	0.18	0.24	0.62
Root Mean Square Error (px)	0.49	0.31	0.41	0.98
CE90 (px / m)	**0.42/1.27**	**0.49/1.47**	**0.68/2.05**	**1.58/4.74**

Table 4-7 Product 5: Salon-de-Provence: Multispectral Band Co-registration Accuracy (Image Matching Confidence Level @ 99 %). Units: Multispectral Pixels.

	Multispectral			
	Band Pair: 1_2	Band Pair: 2_3	Band Pair: 3_4	Band Pair: 4_1
Product 5				
# Matched Pixel Total	4837/20750	4712/20853	198/9370	134/10074
Mean Easting Error (px)	-0.02	0.02	-0.027	-0.19
Mean Northing Error (px)	-0.11	0.19	0.07	0.04
Easting Error Standard Deviation (px)	0.18	-0.06	0.28	0.70

Northing Error Standard Deviation (px)	0.13	0.18	0.29	0.39
Easting Root Mean Square Error (px)	0.18	0.07	0.28	0.73
Northing Root Mean Square Error (px)	0.17	0.26	0.30	0.39
Root Mean Square Error (px)	0.25	0.27	0.41	0.83
CE90 (px / m)	**0.38/1.13**	**0.42/1.27**	**0.70/2.10**	**1.28/3.84**

Table 4-8 Product 1,2 and 5: Salon-de-Provence: Multispectral-Panchromatic Band Co-registration Accuracy (Image Matching Confidence Level @ 99 %). Units: Multispectral Pixels.

	Multispectral-Panchromatic					
	Band Pair: 4_5	**Band Pair: 5_1**	**Band Pair: 4_5**	**Band Pair: 5_1**	**Band Pair: 4_5**	**Band Pair: 5_1**
	Product 1		**Product 2**		**Product 5**	
# Matched Pixel Total	628/12153	592/13050	877/12962	740/15154	398/8959	754/12893
Mean Easting Error (px)	0.28	0.35	0.87	0.62	0.15	0.32
Mean Northing Error (px)	-0.80	-0.21	0.37	0.46	0.11	0.49
Easting Error Standard Deviation (px)	0.99	0.48	0.77	0.48	1.47	0.41
Northing Error Standard Deviation (px)	0.54	0.47	0.54	0.51	1.37	0.45
Easting Root Mean Square Error (px)	1.03	0.59	1.16	0.79	1.47	0.52
Northing Root Mean Square Error (px)	0.96	0.51	0.65	0.68	1.37	0.66
Root Mean Square Error (px)	1.41	0.78	1.33	1.04	2.01	0.84
CE90 (px / m)	**1.84/5.52**	**1.2/3.60**	**1.79/5.36**	**1.49/4.48**	**3.48/10.46**	**1.22/3.66**

The results of the band co-registration accuracy assessment indicate the multispectral bands are reasonably well co-registered, especially when considering the multispectral band co-registration accuracy of data from similar sensors, including Sentinel-2, is CE90 < 0.3 MS pixels [RD-12]. The results also indicate the multispectral-panchromatic band co-registration accuracy is slightly degraded as expected (refined corrections of this nature would only be needed if the data were to be pansharpened but this is not deemed necessary here as pansharpened products are also available to users) but there is room for improvement.

In addition to the above, the error budget is computed (in this case, only for the multispectral bands as an example), and it is based on the rule that per pixel displacement errors are transitive across all band pairs - by summing the displacement for all band pairs (e.g. (1, 2), (2, 3), (3, 4), the result is in the same order of displacement for the band pair (1, 4), as shown in the equation below:

$$D_{1,4} \cong D_{1,2} + D_{2,3} + D_{3,4}$$

Where $D_{1,5}$ stands for displacement between band 1 and 5 (calculated for the easting and northing direction).

By comparing this estimate $D_{1,4}$ against the true value ($D_{4,1}$) obtained with image matching, the error budget of the method is computed (i.e. error budget = $D_{1,4}$ + $D_{4,1}$ or $D_{1,4}$ – $D_{4,1}$); the (average) error budget in the easting and northing directions is 0.14 and 0.08 MS pixels, respectively. These small error budgets indicate that the results are reliable.

Note the product quality metadata files contains information on what appears to be band co-registration accuracy metrics, using a different multispectral band (only) configuration (e.g. band 1_2, band 1_3, where band 1 is the reference band). However, comparisons cannot be made to the results detailed in the tables above, where applicable, as it is not completely clear how these metrics have been calculated or what their units are.

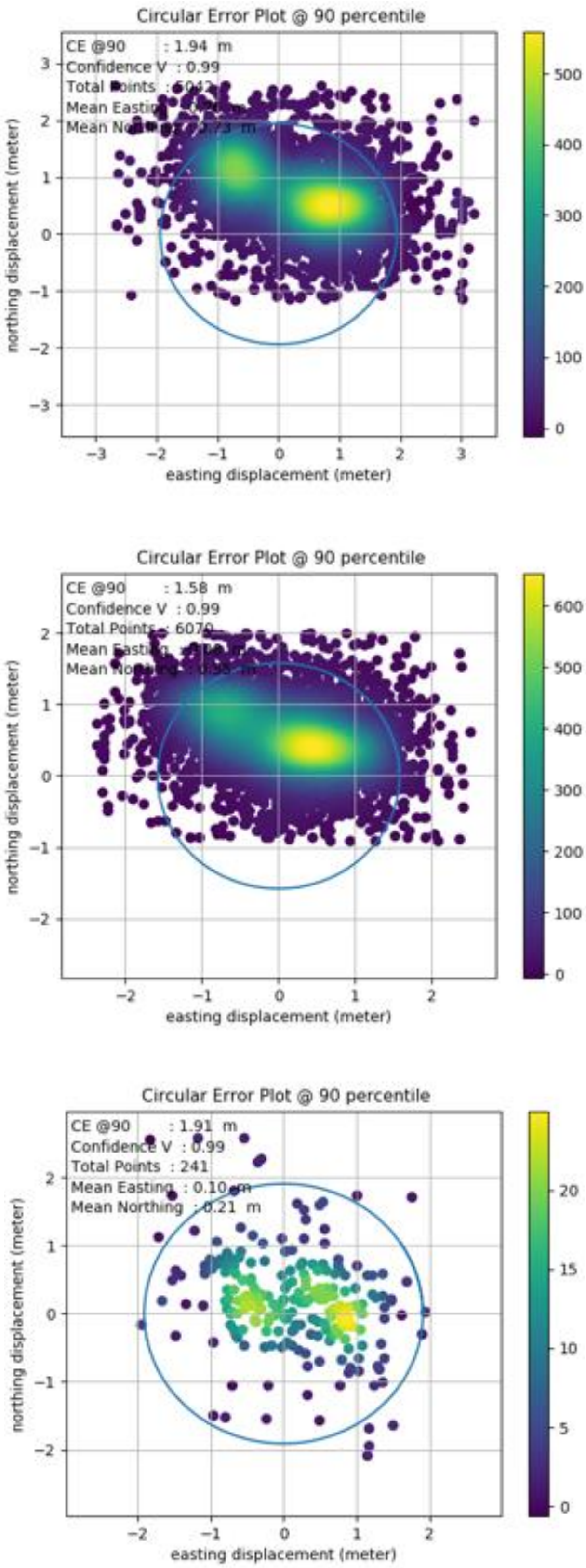

Figure 4-7 Product 1: band 1_2 co-registration accuracy (top), band 2_3 co-registration accuracy (middle) and band 3_4 co-registration accuracy (bottom).

4.3 Radiometric Calibration Quality

This section describes the assessment of radiometric calibration quality of sensor products, detailed in Table 4-9, in terms of **absolute** and **temporal radiometric calibration accuracy**.

Table 4-9: Radiometric Calibration Quality Assessment Product Sample

Location	Product	Product Name (JL1GF02x) L3A
La Crau (France)	1	JL1GF02B_PMS2_20210626180250_200053836_103_0001_001
	2	JL1GF02B_PMS1_20210626180250_200053836_103_0001_001
Gobabeb (Namibia)	6	JL1GF02A_PMS1_20210611162727_200052576_102_0002_001
PICS Libya-4 (Libya)	7	JL1GF02A_PMS1_20191231164155_200020178_104_0005_001
	8	JL1GF02A_PMS1_20210120163244_200038177_103_0002_001

The radiometric calibration, or correction, of sensor data sees to the successful conversion of raw data (i.e. digital numbers) to spectral radiance or reflectance, using coefficients (e.g. physical bias, physical gain, solar spectral irradiance constants) derived pre-flight in laboratory conditions. This is important as it improves the interpretability and quality of the sensor data (and is particularly important when comparing multiple sensor datasets over a period of time, which is commonly performed by the scientific community).

The digital number (DN) to spectral radiance (L) conversion of sensor data, per band (b), is enabled by the following:

$$L_b = (DN_b * GAIN_b) + BIAS_b$$

The spectral radiance (L_b) to top-of-atmosphere reflectance (ρ_b), per band (b) is enabled by the following:

$$\rho_b = \frac{\pi * L_b * d^2}{E_{0b} * Sin(\theta_s)}$$

Where:

E_{0b} is solar spectral irradiance at the sensor for band b (units: $Wm^{-2}\mu m^{-1}$).
θ_s is solar elevation angle at the time / location of acquisition (units: degrees).
d^2 is Sun-Earth distance at the time of acquisition (units: astronomical units).

Note all coefficients mentioned above can be found in the product user guide, the product metadata and online.

4.3.1 Absolute Radiometric Calibration Accuracy

4.3.1.1 Description and Method

The method used to determine the absolute radiometric calibration accuracy of the sensor's bands is based on comparing the top-of-atmosphere (**TOA**) reflectance values derived from the sensors acquisitions of the chosen RadCalNet calibration sites with the TOA reflectance values derived from the RadCalNet calibration sites themselves (i.e. reference TOA reflectance values).

The RadCalNet calibration sites, operated by the CEOS Working Group for Calibration and Validation (**WGCV**) Infrared and Visible Optical Sensors (**IVOS**), provides the scientific community with the following:

- TOA reflectance values, derived from both in-situ surface and atmosphere measurements (e.g. surface pressure, columnar water vapour, columnar ozone, aerosol optical depth, etc.) that are **SI-traceable**, at:
    - 30-minute intervals between 09:00 and 15:00 local standard time (cloud-free data only), and 10 nm spectral sample intervals between 400 nm and 1000 nm.

Note the RadCalNet TOA reflectance values are representative of nadir viewing observations only, so comparison to sensor top-of-atmosphere reflectance values should be used with caution - when the sensor viewing zenith angle deviates significantly from nadir, both atmospheric and surface non-Lambertian behaviour can lead to significant deviation from at-nadir simulated signal. The correction for the latter (i.e. off-nadir viewing angle effects), as well as illumination (solar) angle effects, can be done using bi-directional reflectance modelling.

The products used to assess the absolute radiometric calibration accuracy, by temporal and spectral simulation with RadCalNet data, are the following:

Product 1, 2, 6

These products provide acquisitions of the chosen RadCalNet calibration sites, La Crau (see Table 4-10) and Gobabeb (see Table 4-11). Products providing acquisitions of Baotou and Nevada had also been procured but could not be used in this assessment as RadCalNet data had not been published (or available) for the dates of these acquisitions.

Table 4-10 : RadCalNet La Crau Calibration Site Description

Parameter	Description
Geographic Location	Latitude: 43.558889, Longitude: 4.864167, Altitude: 20 m
Characteristics	The RadCalNet top-of-atmosphere reflectance spectra are representative of a disk of 30 m radius.

Table 4-11 : RadCalNet Gobabeb Calibration Site Description

Parameter	Description
Geographic Location	Latitude: -23.6002, Longitude: 15.1196, Altitude: 510 m
Characteristics	The RadCalNet top-of-atmosphere reflectance spectra are representative of a disk of 30 m radius.

The determined absolute radiometric accuracy cannot be evaluated against a minimum performance requirement as it has not been specified by the operator. Instead, this will be evaluated against what is generally considered very good, based on similar sensors such as Sentinel-2 and Landsat 8 (OLI), which is approximately < 5 % for all bands [RD-12, RD-13].

4.3.1.2 Results

The results of this assessment can be found in Table 4-13 and Table 4-14.

Table 4-12: Jilin-1 GF02A Sensor Observation Conditions (Solar and Viewing Geometries)

Product	Roll Angle / Sensor Viewing Angle (°)	Sensor Azimuth Angle (°)	Solar Elevation Angle (°)	Solar Azimuth Angle (°)	Water Vapour (g/cm)	AOD ()
1	19.57	281.983	61.181	126.604	1.95	0.121
2	19.56	281.504	60.9944	126.265	1.95	0.121
3	-4.30	97.2309	30.4245	41.0399	2.57	0.109

Table 4-13: Jilin-1 GF02A and Simulated Jilin-1 GF02A (RadCalNet) TOA Reflectances

		ρ TOA Reflectance				
Product	**Origin**	**Blue**	**Green**	**Red**	**NIR**	**PAN**
1	Sensor	0.141428	0.146220	0.179746	0.244853	0.177057
	RadCalNet	0.139226	0.144319	0.177102	0.246746	0.177650
2	Sensor	0.132113	0.139293	0.164519	0.230531	0.173571
	RadCalNet	0.139348	0.144597	0.179069	0.248501	0.179542
3	Sensor	0.147722	0.168613	0.240952	0.217243	0.193541
	RadCalNet	0.186915	0.198340	0.260521	0.276210	0.236650

Note the sensor TOA reflectances detailed in the table above have not had directional reflectance corrections applied, especially as the true viewing angle is not available.

The difference, expressed as a percentage, between Jilin-1 GF02A TOA reflectances ($\boldsymbol{\rho_b}\ work$) and simulated Jilin-1 GF02 TOA reflectances ($\boldsymbol{\rho_b}\ simulated$) is calculated as follows:

$$\rho_b = ((\boldsymbol{\rho\_b}\ simulated - \boldsymbol{\rho\_b}\ work)/(\boldsymbol{\rho\_b}\ simulated)) * 100$$

Table 4-14: Comparison between Jilin-1 GF02A and Simulated Jilin-1 GF02A RadCalNet TOA Reflectances

	ρ TOA Reflectance Difference (%)				
Product	**Blue**	**Green**	**Red**	**NIR**	**PAN**
1	-1.51	-1.36	-1.42	0.73	0.33
2	5.19	3.66	8.12	7.23	3.30

3	20.96	14.99	7.51	21.43	0.18

The results of this assessment suggest that the data are poorly calibrated as the absolute radiometric accuracy is generally low and unstable. The cause(s) of the latter is not yet clear, especially as the products assessed have viewing and solar geometries (and atmospheric conditions) within normal or ideal limits, but it may be due to the radiometric calibration method used by the operator [2]– all satellites in the Jilin-1 constellation are cross-calibrated with MODIS (MODIS bottom-of-atmosphere (**BOA**) reflectances propagated to TOA reflectances, using the 6SV radiative transfer model, for acquisitions over China and Africa only). Therefore, it is recommended that the operator re-assess their calibration method.

4.3.2 Temporal Radiometric Accuracy

The temporal radiometric accuracy is determined by producing a time-series of mean TOA reflectance, calculated for a defined area of interest**,** against the number of days since launch. However, this assessment could not be performed as only two products of a suitable site (e.g. Libya-4) were procured.

4.4 Product Image Quality

This section describes the assessment of product image quality on the supplied sensor products in terms of **Signal-to-Noise Ratio** (**SNR**), **Modulation Transfer Function** (**MTF**) and **Image Interpretability**. Table 4-15 details the names of the products used in these assessments.

Table 4-15 Image Quality Assessment Product Sample

Location	Product Number	Product Name (JL1GF02x) L3A
Salon-de-Provence (France)	**5**	**JL1GF02A_PMS1_20210519174421_200050263_105_0005_001_L1**
PICS Libya-4 (Libya)	**7**	**JL1GF02A_PMS1_20191231164155_200020178_104_0005_001**
	8	**JL1GF02A_PMS1_20210120163244_200038177_103_0002_001**

4.4.1 Signal-to-Noise Ratio

4.4.1.1 Description and Method

The SNR is used to quantify the performance of a sensor in response to a particular exposure; it quantifies the ratio of the sensor's output signal to the noise present in the output signal and can be expressed by the following:

[2] When the relative difference between cross-calibration gain coefficients and ground calibration gain coefficients is greater than 10%, the cross-calibration coefficients will replace the ground calibration coefficient [RD-5].

$$SNR = \frac{\mu}{\sigma}$$

Where μ is the mean signal and σ is the standard deviation of the signal.

This assessment was performed on the following products:

Libya-4 (Libya, Africa)

Product 7, 8

This bright desert site is a CEOS Pseudo-invariant Calibration Site (**PICS**), which has been chosen for this particular assessment because it is well known to exhibit reasonable spatial, spectral, and temporal uniformity and has minimal cloud cover. Note the presence of sand dunes in this site does not satisfy the criterion of flat terrain but the method described below accounts for this.

The method proposed for this assessment allows for the estimation of (spatial) SNR, based on the aforementioned equation and the following assumption:

- The mean signal is defined as the spatial average of a group of pixels observing a spatially varying scene and the noise is defined as the standard deviation of this signal for the same group of pixels.

The method, modified since it was initially proposed in [RD-8], is performed for each spectral band, whose imagery has been converted from digital numbers to radiance, in the following way:

1. Compute the local statistics of a small (5 x 5 pixels) sliding window applied to the imagery being assessed. Select only the “best” small windows for the following steps.
    a. The selection of small windows ensures that increased site uniformity is generally maintained (if not, where spatially high frequencies exist (e.g. sharp transitions seen as dune summits, dedicated image processing is applied in order to detect this and filter).

2. Compute the statistical distribution (histogram), between the **minimum** and **maximum radiance**, of the selected “best” small windows (statistics of 5 x 5 pixel windows) – the signal is defined as the peak (i.e. mean radiance) of this statistical distribution and the noise is defined as the standard deviation of this statistical distribution about the mean.

3. Estimate SNR(s).

Note no minimum performance requirement has been specified by the operator for this metric.

Please note that SNR is an important image quality indicator - high SNRs are required in order to control uncertainties in radiometric measurements, especially multispectral bands, as much as possible.

4.4.1.2 Results

The results of this assessment are detailed in Table 4-16.

Table 4-16: SNR Assessment Results

	Product 7			Product 8		
Band	**Mean Radiance W.m-^{2}.str^{-1}**	**Calculated SNR**	**Product Metadata SNR**	**Mean Radiance W.m-^{2}.str^{-1}**	**SNR**	**Product Metadata SNR**
Blue	61.92	213.16	38.43	65.58	202.5	37.85
Green	76.04	217.74	35.54	80.80	172.06	36.77
Red	96.45	159.78	33.83	98.90	137.76	36.59
NIR	68.24	154.17	36.07	73.64	110.71	36.38
PAN	79.11	86.25	38.26	83.33	105.68	38.76

The results of this assessment indicate high SNR values for all bands. Note these SNR values do not compare to those provided in the product metadata but this is most likely due to the different way in which SNR was estimated by the operator (e.g. different method, acquisitions, etc.).

4.4.2 Modulation Transfer Function

4.4.2.1 Description and Method

The modulation transfer function importantly describes the response of the imaging sensor as a function of spatial frequency, and so is strongly related to concepts such as sharpness, contrast and spatial resolution. Therefore, it is considered as an important image quality metric.

(It is important that this image quality metric be monitored post-launch or in orbit, not just pre-launch, in order to ensure that launch vibrations, transitions from air to vacuum, or changes in thermal state, have not degraded the sharpness of the optical imagery.

The product(s) used for this assessment include:

Product 5 (Panchromatic, L1 only)

The metadata of these particular products indicate MTF compensation has not been applied (i.e. if it had been applied, we would expect the results to show an improved MTF).

Note these are basic Level 1 products (operator definition given in Section [RD-3], L0 products are generally not made available externally / publicly) as products generated by higher processing levels commonly include resampling kernels which introduces a smoothing effect and therefore degrades the true MTF.

This assessment has been performed using an open-source tool, validated against third party software, made publicly available at https://github.com/JorgeGIlG/MTF_Estimator. The tool, accompanied by detailed documentation that includes information on the algorithm (Slanted-Edge methodology based) used, works in the following way:

1. Select a band and create a shapefile which defines the target edge to be used:
    a. The target edge must be straight and sharp (a man-made target is more likely to have these features) and defined by uniform high and low reflectance surfaces.
    b. The target edge must be vertical (i.e. the angle is important). This is an important requirement related to how the algorithm works - if an along track or across-track assessment is needed then the image can be rotated accordingly.
2. Run the tool
    a. The data in each transect (each image row), defined by the shapefile, is smoothed and then differentiated in order to obtain a coarse estimation of the pixel position of the target edge. The latter estimation is then used to set the initial conditions of the optimisation technique which is used to fit a sigmoid function to the data (as shown in Figure 4-8).

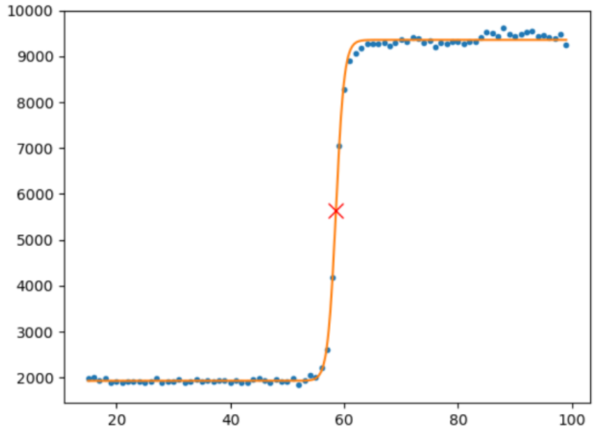

Figure 4-8 The sigmoid function (-) is fitted to the data ( ) in a transect. The point of inflexion (x) shows the estimated sub-pixel edge position. X axis is pixels, y axis is digital numbers

b. The estimated sub-pixel position data for all transects is subjected to linear regression in order to ensure the target edge is straight as assumed (any outliers are removed during this process) and the target edge angle estimated.
c. The estimated sub-pixel edge position is used to shift each transect to a common origin, hence creating a supersampled virtual edge which is modelled as a spline and thus a representation of the Edge Spread Function (**ESF**).
d. The (two-dimensional) Point Spread Function (**PSF**) is obtained by fitting the spline shape to a one-dimensional Gaussian function (Line Spread Function) using Levenberg-Marquardt optimisation.
    i. The PSF defines the apparent shape of a point target as it appears in the resulting image: it is therefore directly related to the sharpness of images provided by the sensor / imaging system.
e. The MTF is then estimated from the modulus of the Fourier transform of the PSF.
    i. The MTF informs on the contrast of the different spatial frequency components of the observed image.

4.4.2.2 Results

This assessment could not be performed as the tool used could not precisely detect or define the edges of the chosen artificial modulation transfer function target (i.e. blurring is evident, poor sharpness indicates degradation of image quality). This may be because the modulation transfer function compensation correction had not been applied during processing, as indicated in the product metadata (this parameter is not sufficiently detailed in [RD-3]).

Note a minimum performance requirement has not been specified by the operator for this metric.

4.4.3 Image Interpretability

4.4.3.1 Description and Method

The image interpretability of optical sensor imagery is an important aspect of image quality (originating from the actual sensor or image processing), especially in terms of their practical use or application. This is commonly assessed, subjectively, using a well-defined procedure that is based on the successful interpretation of objects or features according to the National Imagery Interpretability Rating Scale[3] (**NIIRS**) category in which the sensor belongs [RD-9]. This well-defined procedure also importantly allows for the cross-comparison of image quality from similar sensors.

The products used for this assessment are the following:

Product 5

The method used to assess image interpretability consists of the visual inspection of suitably sized clips of the sensor's imagery, for all bands, centred on the points (objects or features) of interest listed in Table 4-17. If the latter can be successfully detected, at the very least, then image interpretability is considered as good.

Note comparisons are made with clips from a 'gold standard' reference mission (e.g. Pléiades High-Resolution (**PHR**) imagery (bands 1 - 3 only), following downsampling of the spatial resolution to match the spatial resolution of Jilin-1 GF02, also.

The points of interest (**POI**) used for this assessment are defined in Table 4-17. The latter are deemed suitable for **NIIRS Category 3 (2.5 – 4.5 m)** and **NIIRS Category 5 (0.75 – 1.2 m GSD)** [RD-9] imagery.

Table 4-17 POI in Salon-de-Provence.

wkgt_geom (UTM 31)	Id	Description
Point (671090.3105554151115939 4830278.58671295549720526)	1	Modulation Transfer Function target
Point (671364.24309313111007214 4833044.0252351425588131)	2	Motor way / sharp transition (45° NE)
Point (668580.81736886233557016 4828965.45189037173986435)	3	Forest
Point (670056.62237295764498413 4828905.08180973120033741)	4	Roundabout / parking lot
Point (669985.90922565956134349 4832120.72269264236092567)	5	Elevated tree
Point (669956.03863696497865021 4832655.53592716064304113)	6	Motor way / roundabout
Point (670564.24590074480511248 4833363.40447467099875212)	7	The dam
Point (669836.88448120269458741 4832528.00618595350533724)	8	Big building (shadow)
Point (670518.95015854423400015 4829513.56928175128996372)	9	Landing track - 34
Point (670249.72702971810940653 4831735.0312919020652771)	10	Floor painting

[3] *https://fas.org/irp/imint/niirs.htm*

wkgt_geom (UTM 31)	Id	Description
Point (670900.38168655894696712 4829617.21182315889745951)	11	Crop fields / sparse
Point (671548.0352310094749555 4830292.1131860688328743)	12	Broad-leaved woodland
Point (671099.93821095407474786 4828090.14610077627003193)	13	Crop fields
Point (671156.44116920174565166 4828825.77096180152148008)	14	Bridge and water
Point (671120.4438803291413933 4827691.31545618735253811)	15	Crop fields
Point (670328.31568091106601059 4831489.30539688002318144)	16	Building / EA 15
Point (671516.86161747551523149 4833207.41657157335430384)	17	Greenhouse
Point (669996.87127304612658918 4829099.09009433817118406)	18	Parking lot
Point (670062.87681329366751015 4829781.35287734866142273)	19	Plane parking
Point (670860.46870227111503482 4831527.10888031311333179)	20	Plane hangar
Point (671802.47347140731289983 4832385.40385554917156696)	21	Small crop fields
Point (671246.59432400949299335 4832300.03732818737626076)	22	Urban city

4.4.3.2 Results

The primary results generally indicate the image interpretability is reasonable as the POI can be delineated in both the multispectral and panchromatic imagery, as shown in the figures below (this could be improved upon with the reduction of blurring, evident and supported by the preliminary assessment detailed in Section 4.4.2).

Note this assessment takes into account that the contrast is different between the imagery from the two sensors, which is expected as the two sensors have different spectral characteristics, and so is considered as only a minor disadvantage to using this particular method.

(There are some parts of the imagery that appear to be saturated but this is due to the viewing of the imagery quicklooks (subjected to histogram stretching after rescaled to 8-bit) only. The digital numbers have been checked and confirm the latter.)

Band 1 (GF02A, Pléiades, POI 1 - 22)

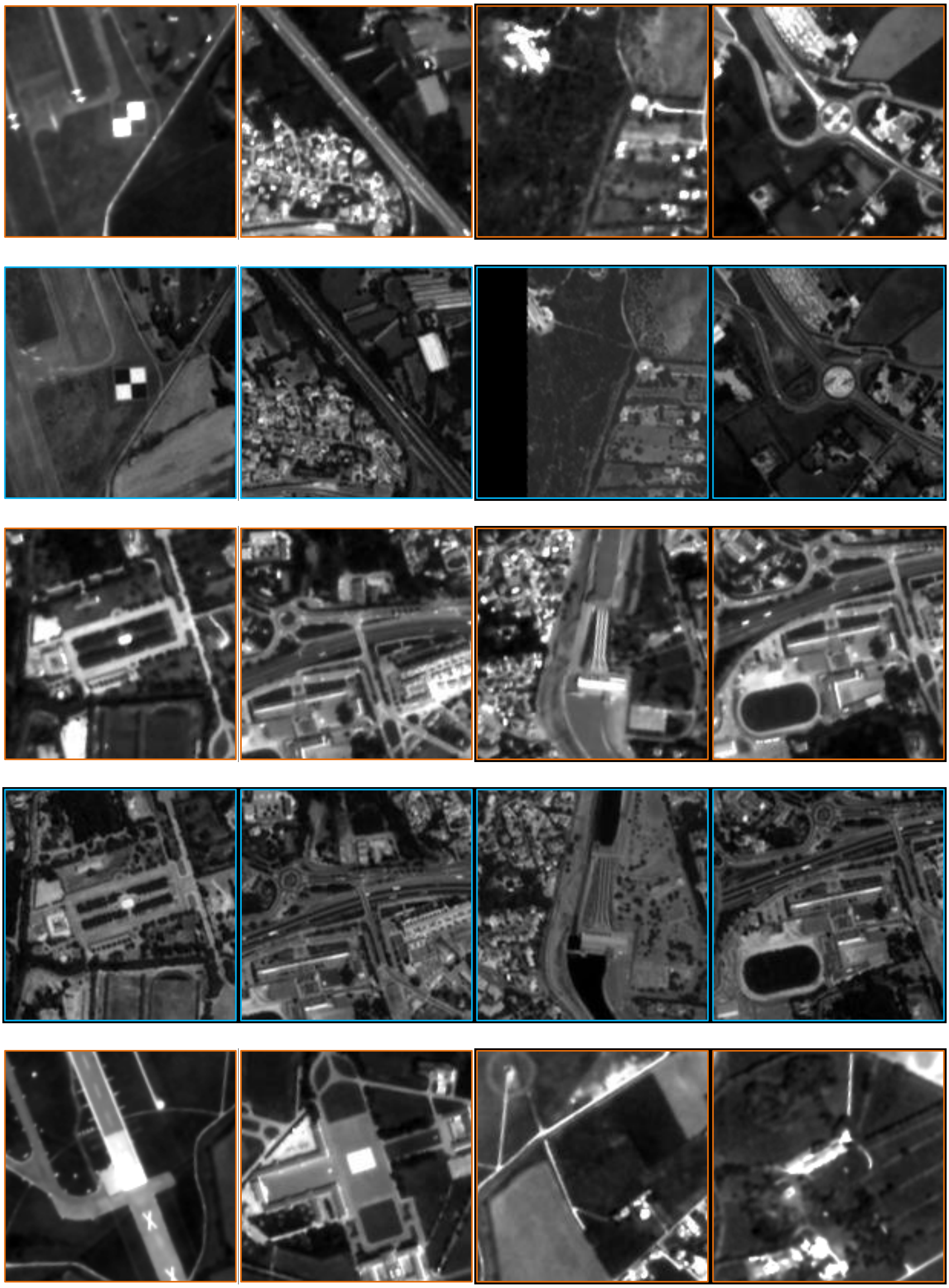

Band 2 (GF02A, Pléiades, POI 1 - 22)

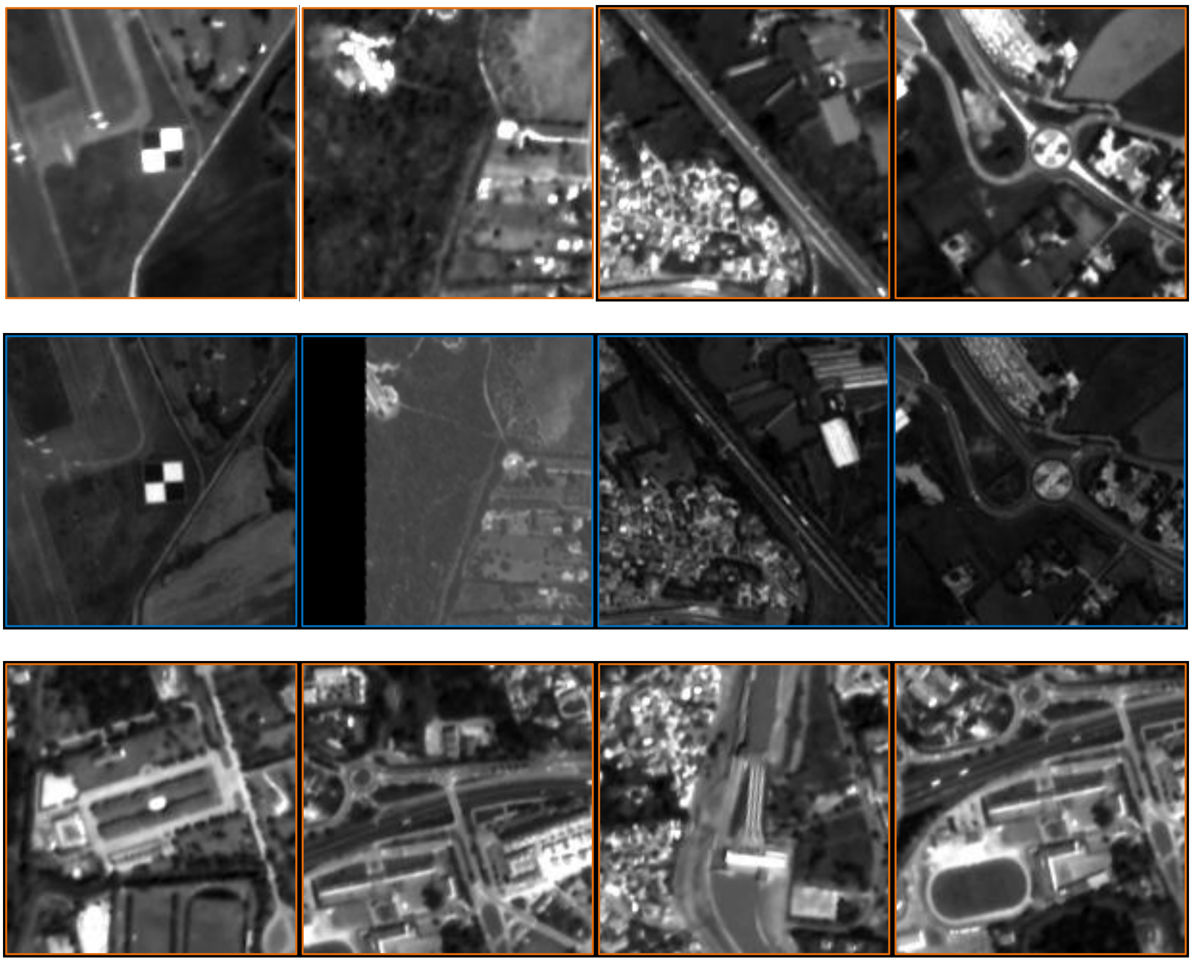

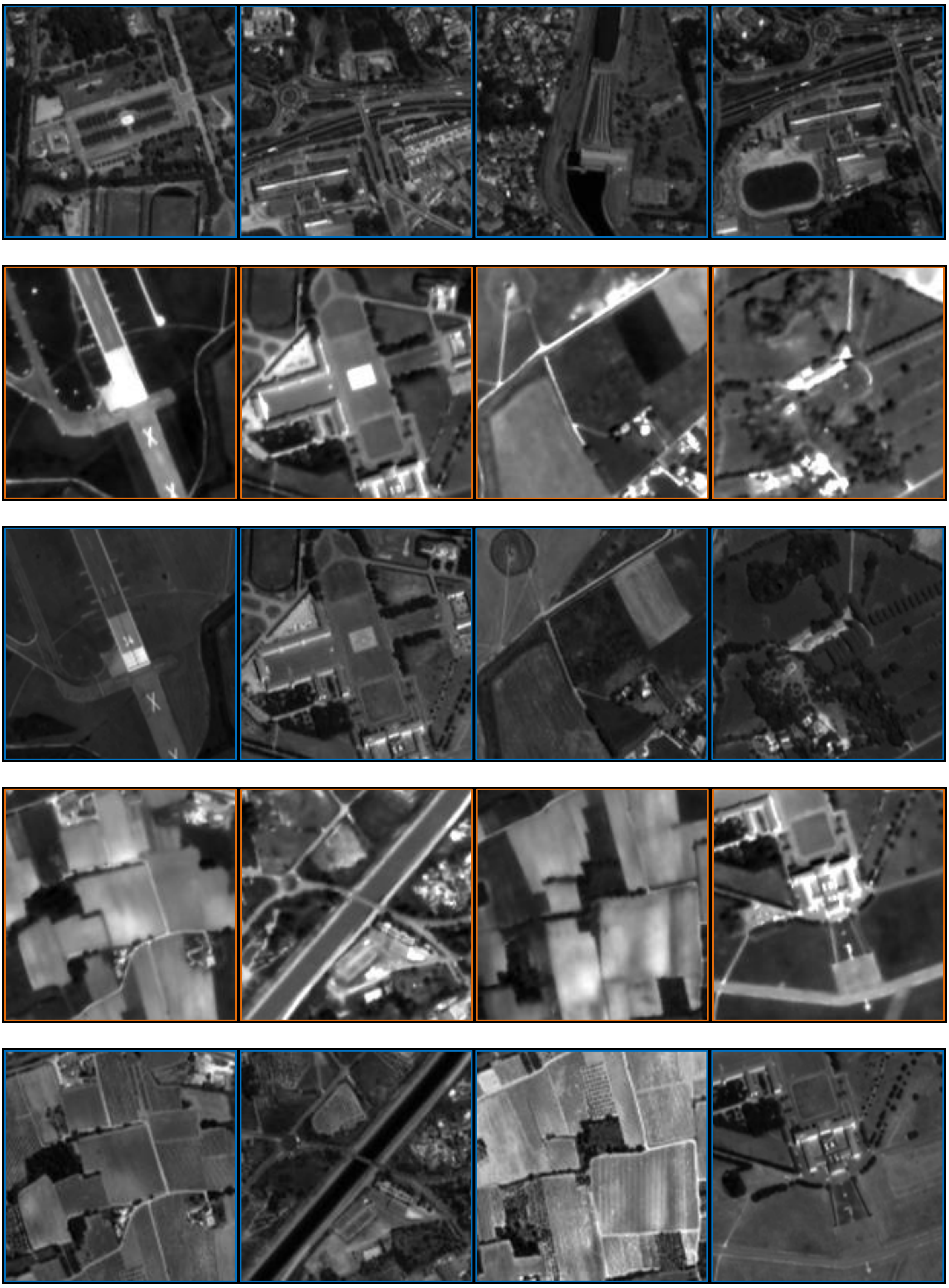

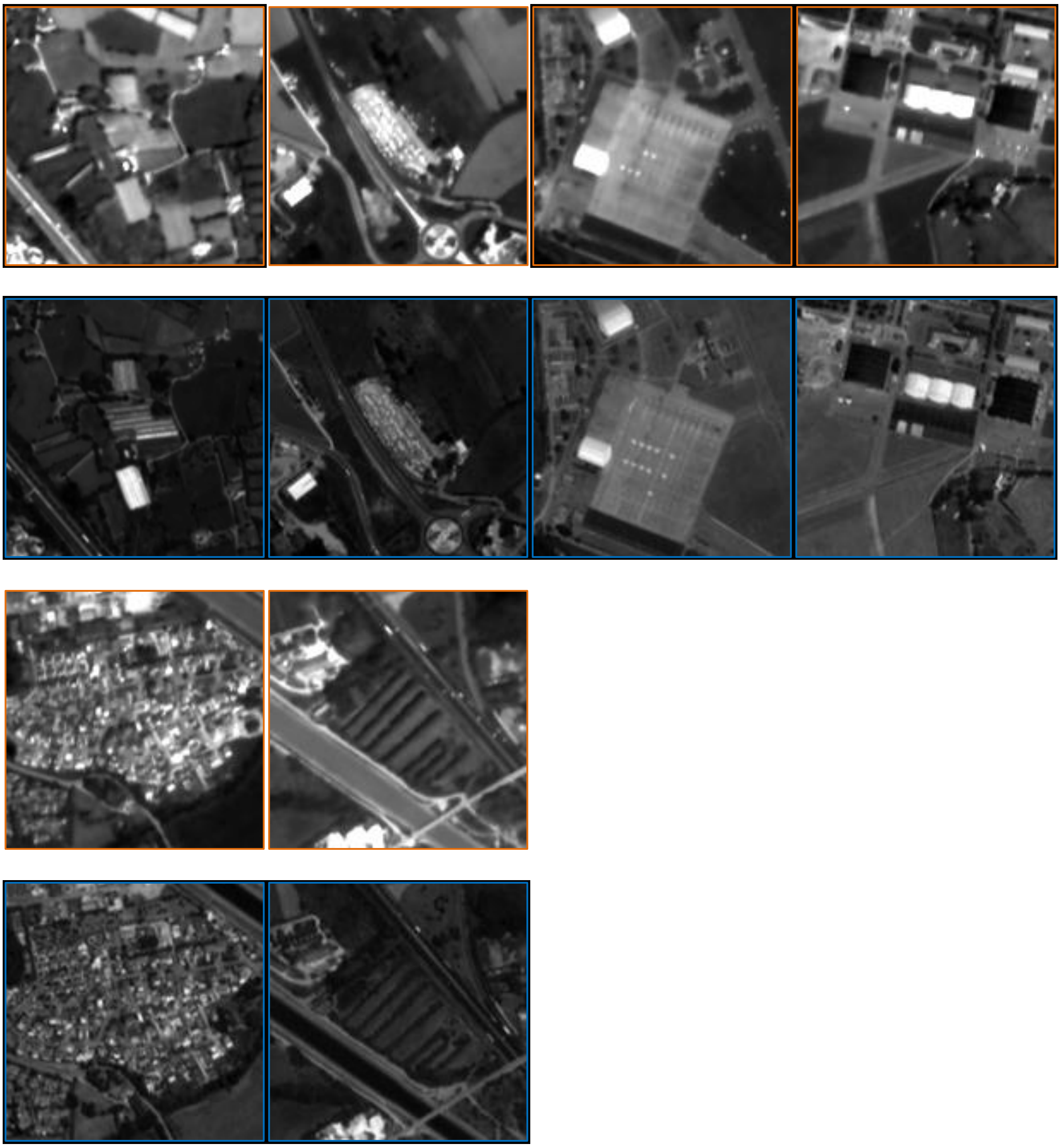

Band 3 (GF02A, Pléiades, POI 1 - 22)

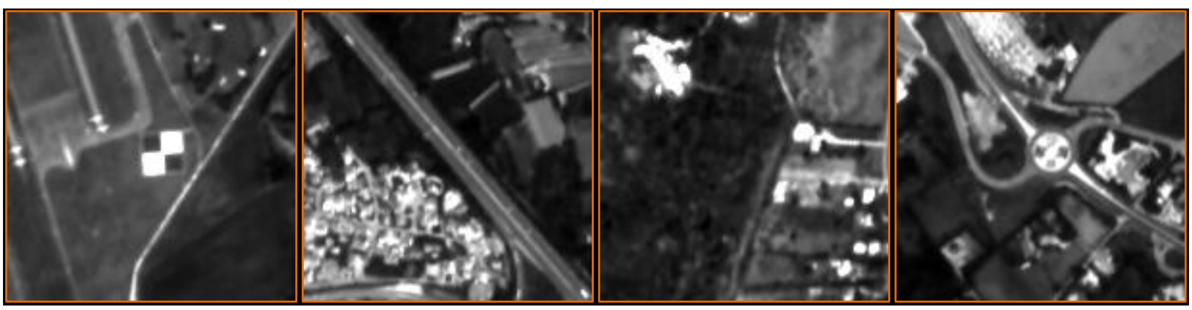

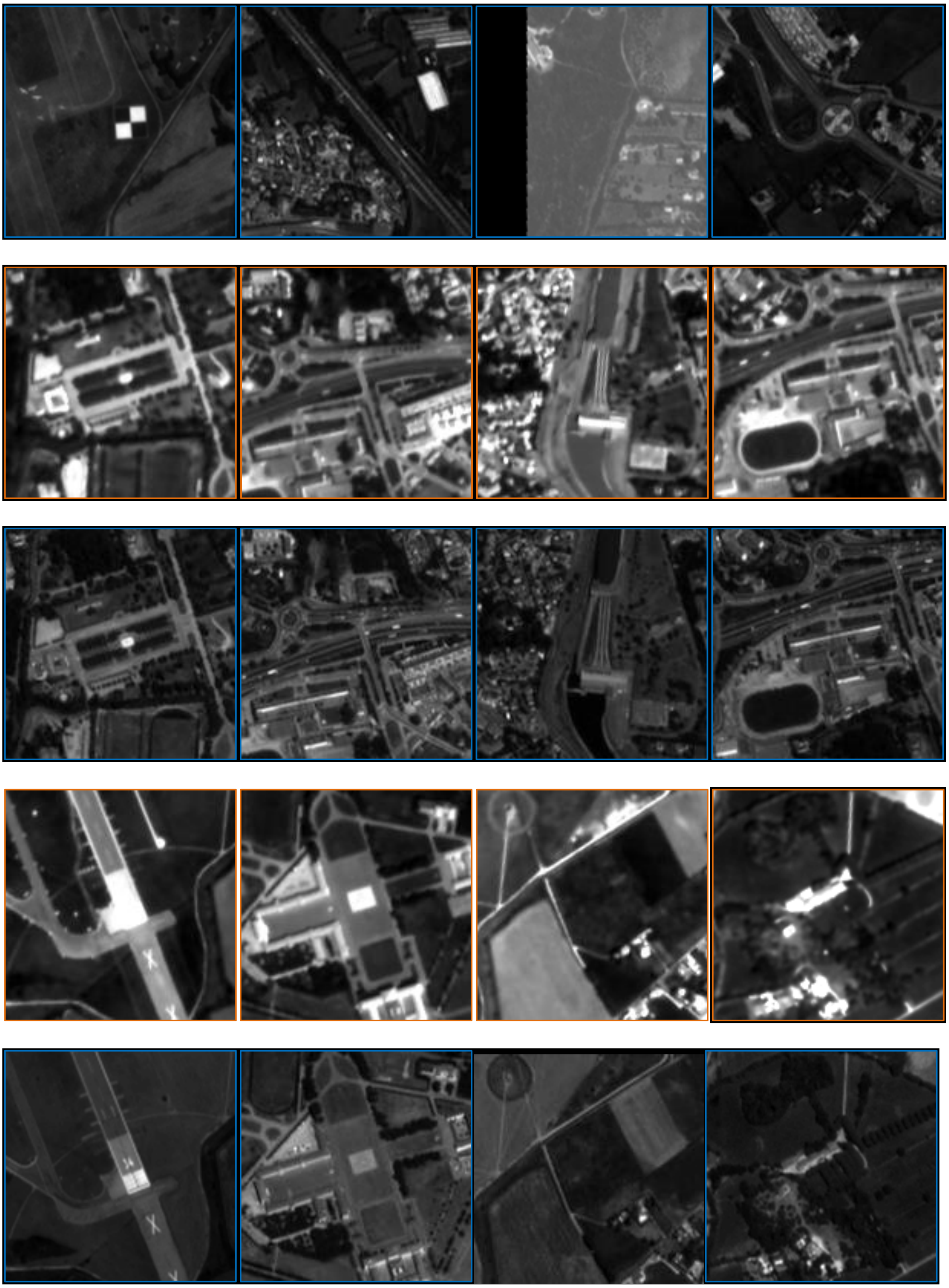

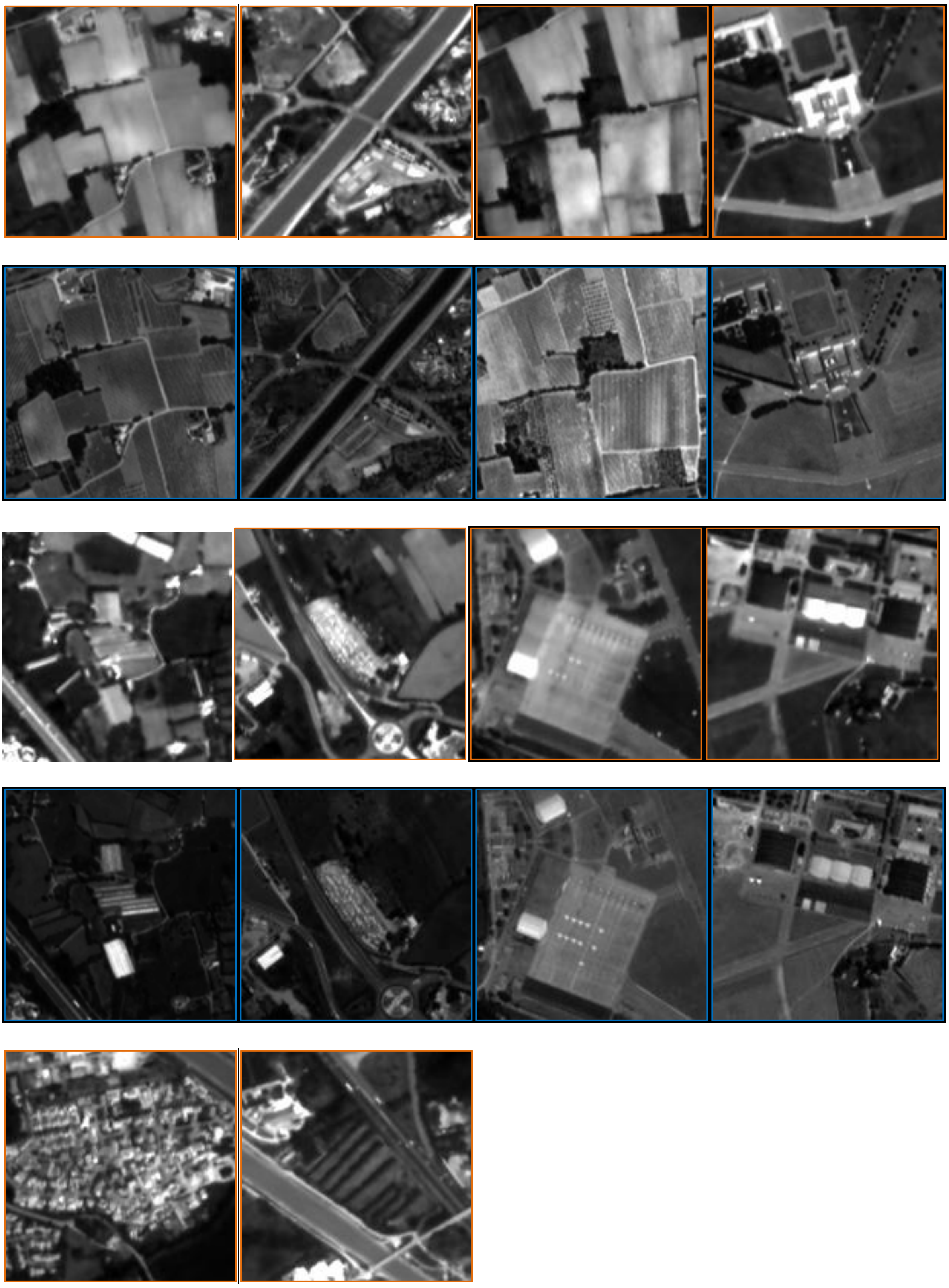

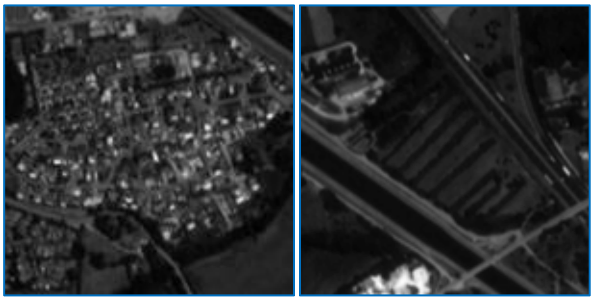

Band 4 (GF02A only, POI 1 - 22)

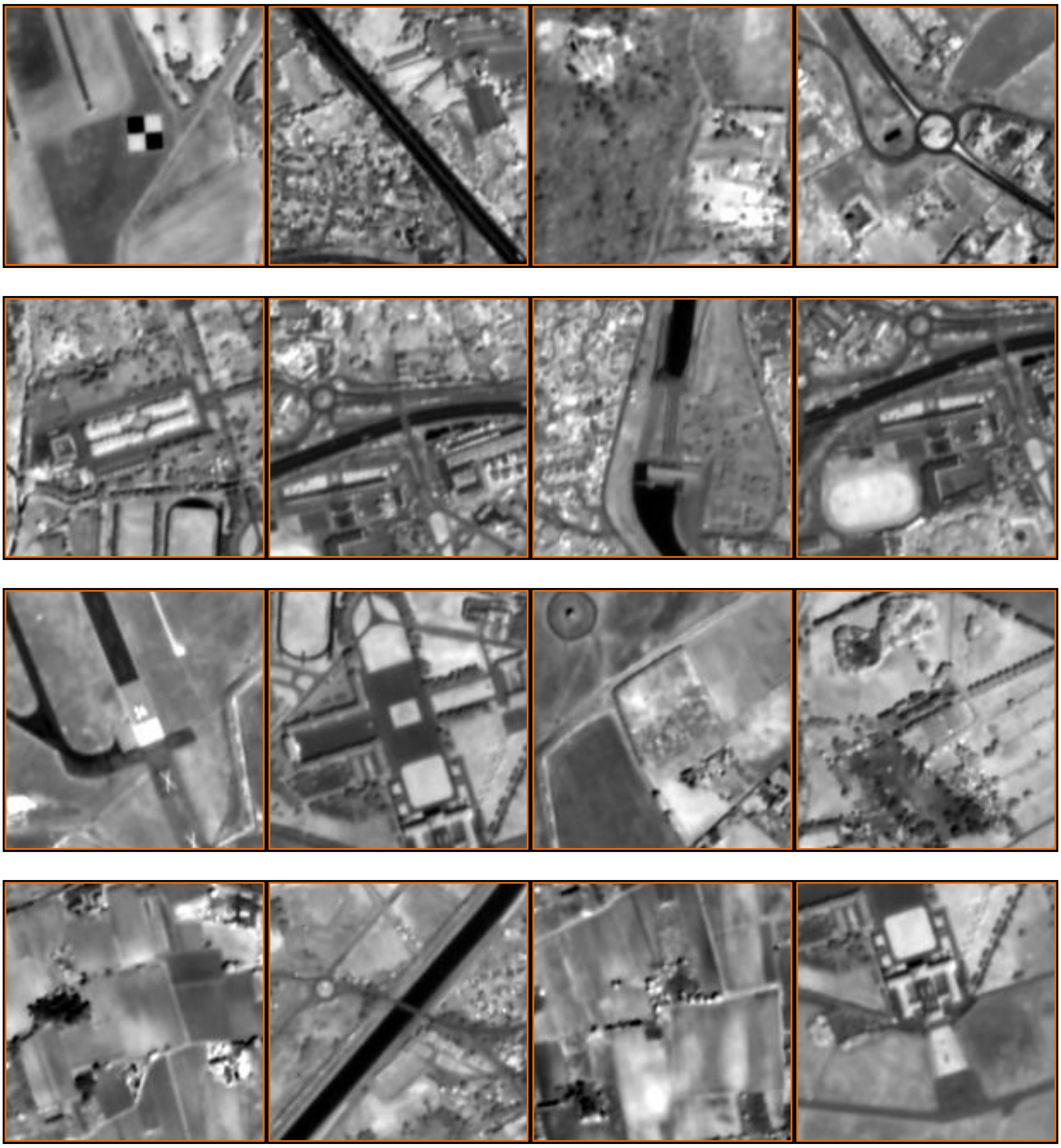

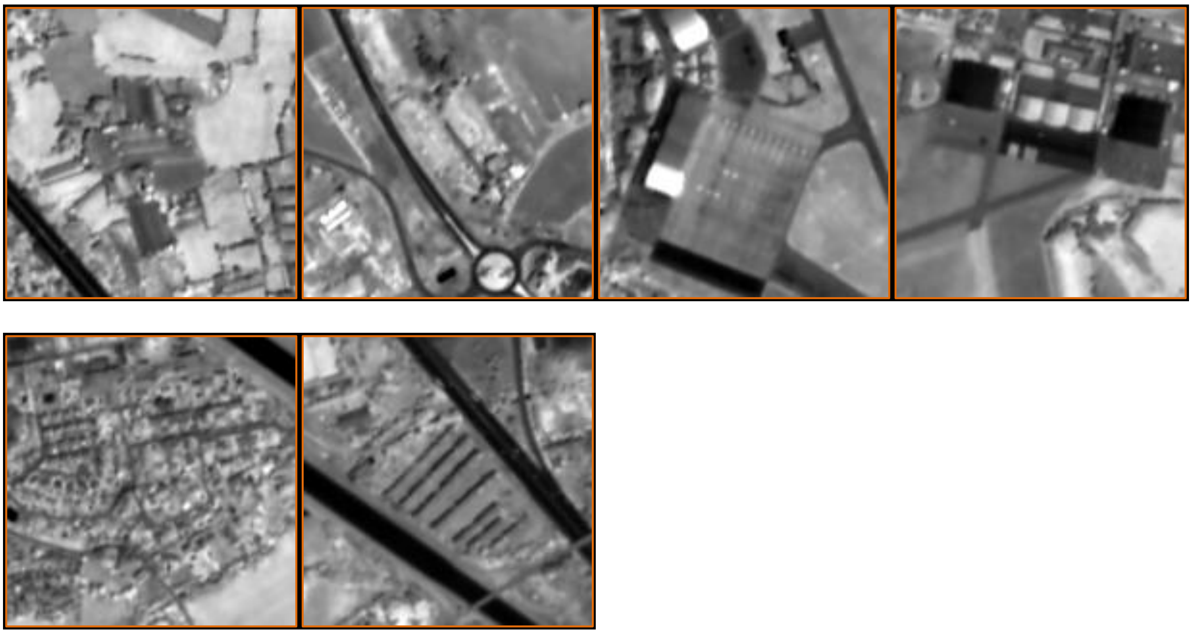

Pan Band (GF02A, POI 1 - 22)

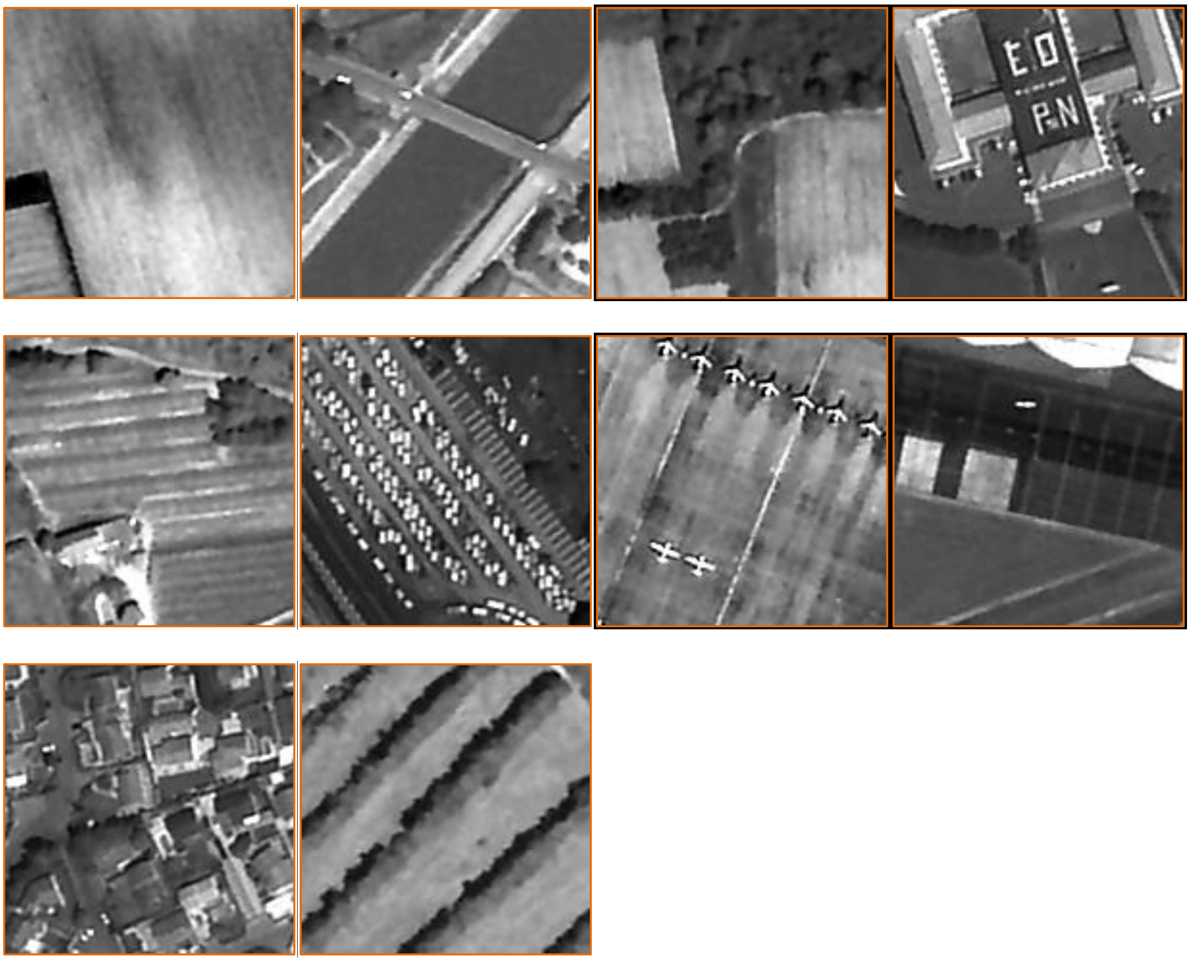

4.5 Visual Inspections

4.5.1 Description and Method

General visual inspections were performed on the multispectral and panchromatic imagery included in all products procured, despite not all being used in the previous assessments, in order to ensure there were no anomalies or artefacts present. The results are detailed in Section 4.5.2.

Note the visual inspections of the product imagery also include inspections of their histograms (e.g. support detection of anomalies or artefacts in the imagery, including saturation) and product metadata (the inspection and extraction of relevant metadata, for example the product quality grade and cloud score, for supporting information despite them not being fully described in the documentation (e.g. how is the product quality grade determined?)).

4.5.2 Results

Product	Visual Inspection Results	
1	PICS Libya-4 (Libya) **Product Name**: JL1GF02A_PMS1_20191231164155_200020178_104_0005_001_L3A **Product Quality Grade**: B **Cloud Score**: 0 (%) **Comment**: The imagery does not appear to contain any anomalies or artefacts. The cloud score appears to be estimated accurately also.	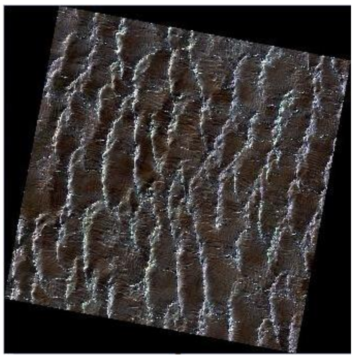
2	PICS Libya-4 (Libya) **Product Name**: JL1GF02A_PMS1_20210120163244_200038177_103_0002_001_L3A **Product Quality Grade**: B **Cloud Score**: 0 (%) **Comment**: The imagery does not appear to contain any anomalies or artefacts. The cloud score appears to be estimated accurately also.	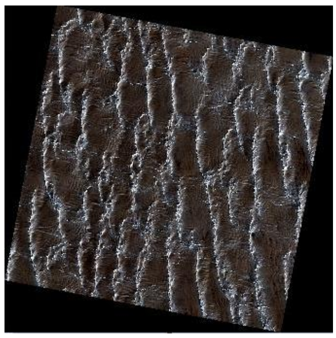

3	Baotou (China) **Product Name**: JL1GF02A_PMS1_20210407104655_200046427_102_0012_001_L3A **Products Quality Grade**: A **Cloud Score**: 0 (%) **Comment**: The imagery does not appear to contain any anomalies or artefacts. The cloud score appears to be estimated accurately also.	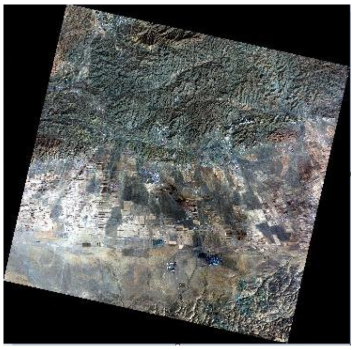
	Baotou (China) **Product Name**: JL1GF02A_PMS2_20210429105710_200048406_101_0007_001_L3A **Products Quality Grade**: A **Cloud Score**: 0 (%) **Comment**: The imagery does not appear to contain any anomalies or artefacts. The cloud score appears to be estimated accurately also.	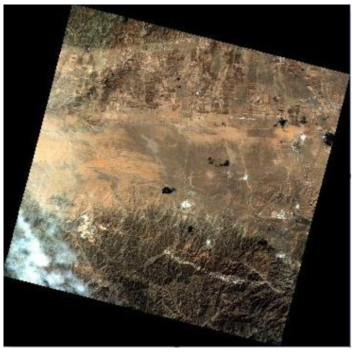
4	Piedmont (Italy) **Product Name**: JL1GF02A_PMS1_20210403174102_200046065_101_0002_001_L3A **Products Quality Grade**: A **Cloud Score**: 0 (%) **Comment**: The imagery does not appear to contain any anomalies or artefacts. The cloud score appears to be estimated accurately also.	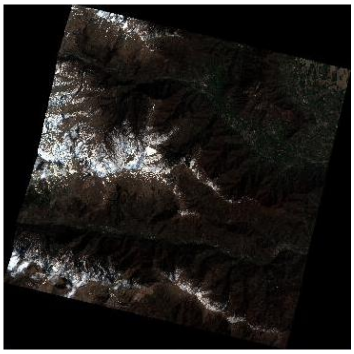
5	Piedmont (Italy) **Product Name**: JL1GF02A_PMS1_20210413175418_200046999_102_0002_001_L3A **Products Quality Grade**: A **Cloud Score**: 10 (%) **Comment**: The imagery does not appear to contain any anomalies or artefacts. The cloud score appears to be estimated accurately also.	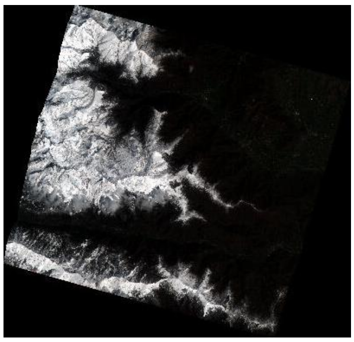

6	Gobabeb (Namibia) **Product Name**: JL1GF02A_PMS2_20201217163447_200035870_102_0021_001_L3A **Products Quality Grade**: A **Cloud Score**: 8 (%) **Comment**: The imagery does not appear to contain any anomalies or artefacts. The cloud score may be overestimated as the very light-coloured surface geology, composed of calcisols and gypsisols, of this area is predominant in this acquisition and might be mistaken for cloud in the calculation of the cloud score. (It is important to mention that this desert, which is known as a unique coastal fog desert, experiences morning fog (caused by cold currents in the Atlantic cooling the air just above the water, and then the winds blowing the cooled air inland and over the hot desert) on a near daily basis but then if this were the case then you would expect to see it cover the orange coloured Namib Sand Sea also.)	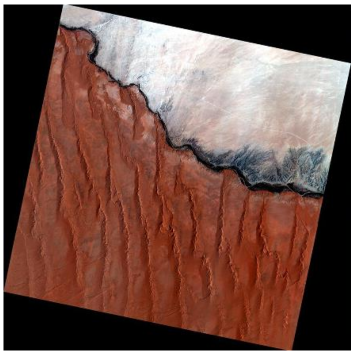
8	Gobabeb (Namibia) **Product Name**: JL1GF02A_PMS1_20210519174421_200050263_105_0005_001_L3A **Product Quality Grade**: A **Cloud Score**: 0 (%) **Comment**: The imagery does not appear to contain any anomalies or artefacts. The cloud score appears to be estimated accurately also.	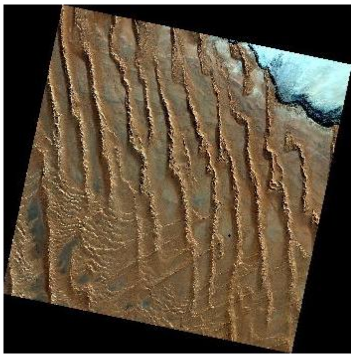
8	Salon-de-Provence (France) **Product Name**: JL1GF02A_PMS1_20210519174421_200050263_105_0005_001_L3A **Product Quality Grade**: B **Cloud Score**: 0 (%) **Comment**: The product imagery does not appear to contain any anomalies or artefacts. However, the cloud score appears to be underestimated (cloud is clearly evident in the acquisition).	

9	La Crau (France) **Product Name:** JL1GF02B_PMS1_20210626180250_200053836_103_0001_001 **Product Quality Grade**: A **Cloud Score**: 0 **Comment**: The imagery does not appear to contain any anomalies or artefacts. The cloud score appears to be estimated accurately also.	
10	La Crau (France) **Product Name:** JL1GF02B_PMS2_20210626180250_200053836_103_0001_001_L3A **Product Quality Grade**: A **Cloud Score**: 0 **Comment**: The imagery does not appear to contain any anomalies or artefacts. The cloud score appears to be estimated accurately also.	

5. CONCLUSIONS

This technical note details the preliminary data quality assessments (including geometric calibration, radiometric calibration and image quality) performed on a very small sample of **orthorectified Jilin-1 GF02 bundle products**. The results of the aforementioned data quality assessments generally indicate the **performance of the sensor and the processing implemented is relatively good**. It is, however, recommended that the data provider / operator address, at the very least, the following:

- The provision of more accurate product metadata (e.g. viewing angle).
- The provision of more detailed documentation / user guide (e.g., the quality metadata file is a definite asset to the product but unfortunately, the contents are not adequately described and so the metadata cannot be used reliably or in the correct context).
- The provision of minimum performance requirements so that it is clear to users what level of quality, especially geometrically and radiometrically, can be guaranteed or expected.
- The method used for radiometric calibration should be re-assessed by the operator, for the reasons described in relevant section of this technical note.

Please note the very small sample of products assessed meant that that no comments could be made on items such as general stability (temporal assessments) or consistency across both satellites.

APPENDIX A JILIN-1 GF02A TEST DATASET

Table 5-1: Test dataset used for the analysis of Jilin-1 GF02A

Site	Product Type	Product_Identifier
La Crau (France)	Non-Ortho L1 Product MSS & PAN	**JL1GF02B_PMS1_20210626180250_200053836_103_0001_001**
La Crau (France)	Non-Ortho L1 Product MSS & PAN	**JL1GF02B_PMS2_20210626180250_200053836_103_0001_001**
Piedmont (Italy)	Non-Ortho L1 Product MSS & PAN	**JL1GF02A_PMS1_20210403174102_200046065_101_0002_001**
Piedmont (Italy)	Non-Ortho L1 Product MSS & PAN	**JL1GF02A_PMS1_20210413175418_200046999_102_0002_001**
Salon-de-Provence (France)	Non-Ortho L1 Product MSS & PAN	**JL1GF02A_PMS1_20210519174421_200050263_105_0005_001**
Gobabeb (Namibia)	Non-Ortho L1 Product MSS & PAN	**JL1GF02A_PMS1_20210611162727_200052576_102_0002_001**
Libya-4 (Libya)	Non-Ortho L1 Product MSS & PAN	**JL1GF02A_PMS1_20191231164155_200020178_104_0005_001**
Libya-4 (Libya)	Non-Ortho L1 Product MSS & PAN	**JL1GF02A_PMS1_20210120163244_200038177_103_0002_001**

[END OF DOCUMENT]